

Laser-induced migration and isotope separation of epi-thermal monomers and dimers in supercooled free jets

JEFF W. EERKENS

CRISLA Research Laboratory, Nuclear Science and Engineering Institute, University of Missouri, Columbia, Missouri

(RECEIVED 9 March 2004; ACCEPTED 10 August 2004)

Abstract

Explicit relations are developed to estimate the outflux of migrating isotopomers ${}^i\text{QF}_6$ to the outskirts of a supersonic supercooled free jet whose core is irradiated by a co-axial laser beam and intercepted by a skimmer that separates core gas from peripheral gases. The QF_6 target gas is diluted in carrier gas G ($G = \text{He}, \text{N}_2, \text{Ar}, \text{Xe}, \text{SF}_6$, etc.) which determines the jet's supersonic characteristics and forms $\text{QF}_6\text{:}G$ dimers at low temperatures. Under isotope-selective laser excitation, excited ${}^i\text{QF}_6^*$ convert their vibrational energy V into kinetic energy T after forming transient ${}^i\text{QF}_6^*\text{:}G$ dimers that dissociate in sub-microseconds. Three migrating groups with different transport parameters are created in the jet: thermal monomers, faster-moving epithermal monomers, and slower-moving dimers. Jet-core-fleeing QF_6 is enriched in ${}^i\text{QF}_6$ due to enhanced outwards migration of ${}^i\text{QF}_6^!$ epithermals and reduced escape of ${}^j\text{QF}_6\text{:}G$ dimers in the jet. Isotope enrichments in the rim gases are highest for heavier carrier gases such as $G = \text{Xe}$ or $G = \text{SF}_6$.

Keywords: Epithermal molecules; Laser isotope separation; Monomer versus dimer migration rates; SF_6 and UF_6 ; Supersonic free jets

1. INTRODUCTION

The present paper is a sequel to Eerkens (1998), providing more complete calculations of dimer-mediated isotope enrichment effects from vibrationally laser-excited ${}^i\text{QF}_6$ molecules in supercooled gas streams. The laser-irradiated QF_6 vapor ($Q = \text{S}, \text{Se}, \text{Te}, \text{Mo}, \text{W}, \text{U}$, etc.) is dispersed through carrier gas G (e.g., $G = \text{H}_2, \text{He}, \text{N}_2, \text{Ar}, \text{Xe}, \text{SF}_6, \text{SiBr}_4$) with which it can form $\text{QF}_6\text{:}G$ dimers, and is supercooled by supersonic expansion in a free jet. In molecular laser isotope separation (MLIS) applications, ${}^i\text{QF}_6$ isotopomers are then selectively excited via their ν_3 vibrational absorption bands that are isotope-shifted from those of ${}^j\text{QF}_6$ species.

In one MLIS scheme employing supersonic free jets, jet-fleeing ${}^i\text{QF}_6$ molecules are harvested after excited ${}^i\text{QF}_6^*\text{:}G$ dimer predissociations and VT conversions take place, and formation of non-excited ${}^i\text{QF}_6\text{:}G$ is reduced relative to ${}^j\text{QF}_6\text{:}G$ dimers (Lee, 1977; VandenBergh, 1985; Eerkens, 1998). After passage through an irradiation chamber, the jet enters a skimmer that separates the jet's core flow from peripheral gases which are pumped out separately as

shown in Figure 1. This MLIS harvesting concept was first conceived by Y.T. Lee (1977). Lee originally proposed to directly excite and dissociate already dimerized species such as $\text{QF}_6\text{:}G$ or $(\text{QF}_6)_2$. However excitation of QF_6 monomers, which subsequently dimerize and predissociate in the same manner is more effective (Eerkens, 2001a). An advantage of the latter scheme is that monomers have stronger absorption peaks than dimers. Below 20 K however long-lived dimerization dominates, and only direct laser excitation of dimers can induce isotope separation.

The kinetics of transient $\text{QF}_6^*\text{:}G$ dimer bondings and predissociations with VT conversion was investigated experimentally by VandenBergh (1985). This mechanism has a much higher VT conversion probability at low temperatures and pressures than direct specular VT conversions, and provides the basis for MLIS processes employing dimer harvesting, named SILARC (Separation of Isotopes by Laser Assisted Repression of Condensation) or CRISLA (Condensation Repression by Isotope Selective Laser Activation) (Eerkens, 1998). Earlier experiments in the 1970s through 1980s had shown pre-dissociation lifetimes of laser-excited dimers to be $\tau_{\text{pd}} < 10^{-6}$ s for internal ν_3 infrared vibrations in $\text{QF}_6^*\text{:}G$ or $\text{QF}_6^*\text{:}\text{QF}_6$ dimers. Measured dimer absorption bands of these internal vibrations showed center frequencies

Address correspondence and reprint requests to: Jeff W. Eerkens, University of Missouri, Nuclear Science and Engineering Institute, CRISLA Research Laboratory, Columbia, MO 65211. E-mail: eerkensj@missouri.edu

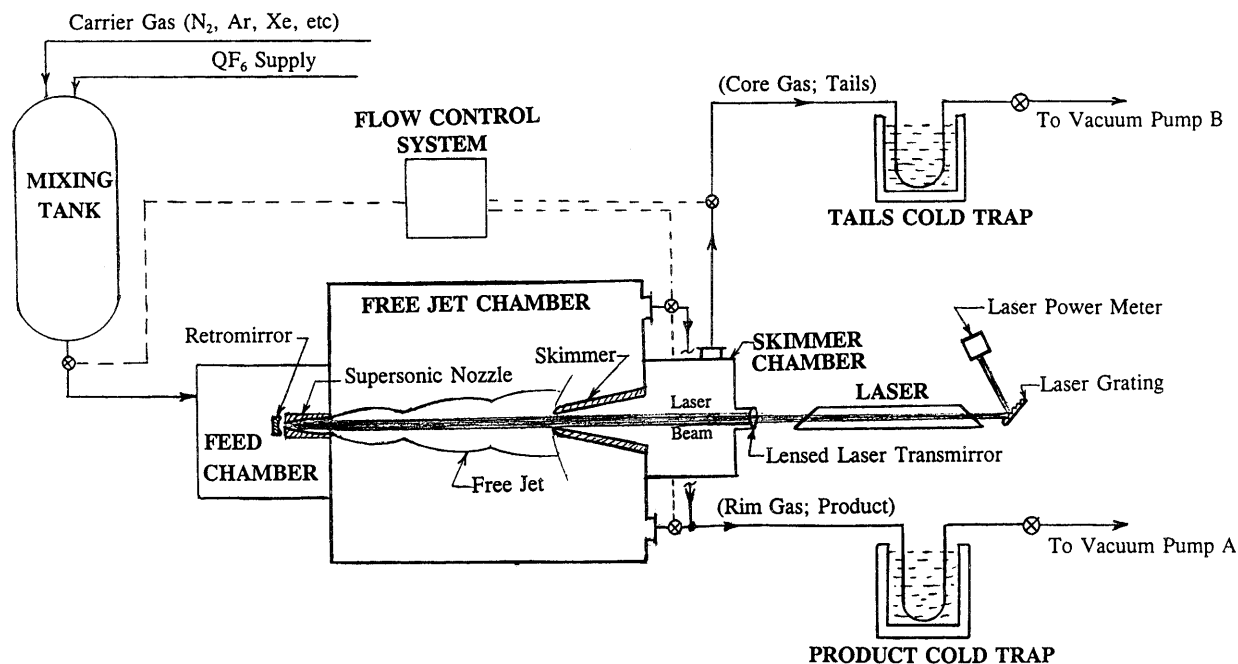


Fig. 1. Schematic of CRISLA chamber with free jet and skimmer.

that were slightly red- (and blue-) shifted from the monomer ν_3 frequency. With broadened widths inversely proportional to predissociation lifetimes, one deduced $\tau_{pd} < 10^{-6}$ s (Smalley *et al.*, 1976; Beswick & Jortner, 1978; Bernstein & Kolb, 1979; Geraedts *et al.*, 1981, 1982; Snells & Reuss, 1987; Liedenbaum *et al.*, 1989; VanBladel & VanderAvoird, 1990; Beu & Takeuchi, 1995, 1997; Beu *et al.*, 1997; McCafferey, 2002).

Although most earlier measurements were made with laser excitation of initially unexcited dimers, if an already ν_3 -excited QF_6^* monomer forms a $\text{QF}_6^*:\text{G}$ or $\text{QF}_6^*:\text{QF}_6$ dimer, the latter should dissociate at essentially the same rate as a direct-dimer-excited species would. Internally excited $\text{QF}_6(\nu_3)^*$ molecules move at the same translational speeds as unexcited QF_6 and should dimerize at the same pace. Because of the large frequency difference of internal ν_3 vibrations and dimer-bond vibrations ν_α , there is initially no coupling between these vibrations during dimer formation. After dimer bonding and a few dimer rotations and bond vibrations, predissociation with VT conversion of ν_3 ensues in a Lissajous excursion. The small frequency defect $\Delta\nu_3$ between internal ν_3 vibrations of monomers and dimers to be accommodated during dimer formation, may aid the predissociation process. Dimerization, previously thought to require three-body collisions (Hirschfelder *et al.*, 1967), actually proceeds much faster by two-body collisions (Eerkens, 2001a). This coupled with the discovery of microsecond lifetimes for excited $\text{QF}_6^*:\text{G}$ dimers, correctly explains and predicts CRISLA isotope separations.

VandenBergh (1985) observed isotope-selective effects from predissociation and VT conversion of $\text{SF}_6(\nu_3)^*:\text{Ar}$,

after SF_6 monomers were excited and subsequently formed $\text{SF}_6^*:\text{Ar}$ dimers. He also investigated and compared such effects for directly laser-excited $\text{SF}_6^*:\text{Ar}$ dimers. Both excitation schemes gave similar results, except that monomer excitations gave higher yields, attributable to the fact that photon absorption resonances for monomers are sharper and stronger. Since $\tau_{pd} < 10^{-6}$ sec and dimer formation times τ_{df} and jet transit times t_{tr} exceed 10^{-6} sec, the time τ_{dVT} to produce a VT conversion after a $\text{QF}_6(\nu_3)^*:\text{G}$ dimer forms, is essentially instant compared to other microscopic processes in the jet; that is $\tau_{dVT} = \tau_{df} + \tau_{pd} \approx \tau_{df}$.

The pathways by which an internal vibration in excited gaseous QF_6^* can relax are:

1. Spontaneous (Einstein) Photon Emission (lifetime $\tau_{se} = \mathcal{A}_{se}^{-1}$)
2. Direct collisional VT conversion (lifetime $\tau_{VT} = k_{VT}^{-1}$)
3. Direct collisional (near-)resonant VV transfer (lifetime $\tau_{VV} = k_{VV}^{-1}$)
4. Transient excited dimer formation followed rapidly by predissociation (lifetime $\tau_{df} = k_{df}^{-1}$)

In MLIS one needs to know how fast mechanisms 1 through 4 are, compared to:

5. Dimer dissociation lifetimes of non-excited dimers (τ_{dd})
6. Transit time of the jet through the laser irradiation cell (t_{tr})

The transit time by a jet traversing a laser beam equals:

$$t_{tr} = L/\bar{U}, \quad (1)$$

where L is the distance traveled by the gas through the laser irradiation region and \bar{U} is the average flow velocity of the jet in the absorption cell. Typically, $2 < L < 20$ cm, and $0.1 < \bar{U} < 2$ km/s, so $10^{-5} < t_{tr} < 2 \times 10^{-3}$ s. In the gas phase, only options (1) through (4) are available to excited QF_6^* molecules for V-relaxation. For V-excited monomers that adsorb or condense on a surface, mechanisms (1)–(4) still apply with some modification, but in addition one must include interactions with phonons in the condensate which populate the latter's internal energy reservoirs. This situation (cold surface condensation) is examined in a separate paper (Eerkens, 2002). The analyses provided in that paper and in the present one, supersede and correct the theory given in Section 2 of (Eerkens, 1998).

We first examine probabilities and rates of processes (1) through (5), and then obtain enrichment parameters for the lightest and heaviest hexafluoride, SF_6 and UF_6 . These molecules possess desirable isotopes ^{33}S (0.74% ab.) used to generate ^{33}P for nuclear medicine, and ^{235}U (0.71% ab.) used as fuel for nuclear reactors. $^{33}\text{SF}_6$ can be excited by the 10P-26 and 10P-28 lines of the CO_2 laser, while $^{235}\text{UF}_6$ is excitable with 16-micron rapidly pulsed Raman-converted CO_2 laser photons or by 5-micron CO laser photons (VandenBergh, 1985; Eerkens, 1998).

2. INTERACTIONS OF QF_6 WITH PHOTONS

2.1. Laser excitation of QF_6

The laser excitation rate k_A for $^i\text{QF}_6$ molecules to absorb resonant laser photons equals:

$$k_A = \varphi_L \sigma_A, \text{ s}^{-1} \text{ per } ^i\text{QF}_6 \text{ molecule}, \quad (2)$$

where σ_A is the laser photon absorption cross-section (cm^2). QF_6 absorption bands are hot-band-broadened, their peaks becoming sharper and higher towards lower temperatures. The laser flux φ_L is given by:

$$\varphi_L = 5.035 \times 10^{22} I_L (\text{W}/\text{cm}^2) / \epsilon_L (\text{cm}^{-1}), \text{ photons } \text{cm}^{-2} \text{ s}^{-1}. \quad (3)$$

Here I_L is the laser beam intensity in Watts/ cm^2 and $\epsilon_L = h\nu_L$ the laser photon energy in cm^{-1} . Typical vibrational absorption cross-sections have (temperature-dependent) values on the order of $\sigma_A \approx 10^{-18} \text{ cm}^2$ at $T < -150$ K near a fundamental band peak (e.g., the ν_3 vibration of QF_6), $\sigma_A \approx 10^{-20} \text{ cm}^2$ for binary combination bands (e.g., the $\nu_2 + \nu_3$ vibration of QF_6), and $\sigma_A \approx 10^{-22} \text{ cm}^2$ for tertiary $\text{QF}_6(3\nu_3)$ absorptions. The laser photon energy ϵ_L must of course be equal to the vibrational excitation quantum ϵ_a (or $\epsilon_a + \epsilon_b, 3\epsilon_a$) to effect resonant absorptions. For the ν_3 vibration of $^{33}\text{SF}_6$ one has $\epsilon_L \approx \epsilon_3 \approx 939 \text{ cm}^{-1}$ and $\sigma_A(\nu_3) \approx 2 \times 10^{-18} \text{ cm}^2$, while for $^{235}\text{UF}_6$ it is $\epsilon_L \approx \epsilon_3 \approx$

628.3 cm^{-1} and $\sigma_A(\nu_3) \approx 10^{-18} \text{ cm}^2$. Then Equation (2) yields:

$$k_A = 106.2 I_L (\text{W}/\text{cm}^2), \text{ s}^{-1} \text{ per } ^{33}\text{SF}_6 \text{ molecule, with} \\ \epsilon_L = 939 \text{ cm}^{-1} \quad (4)$$

$$k_A = 80.2 I_L (\text{W}/\text{cm}^2), \text{ s}^{-1} \text{ per } ^{235}\text{UF}_6 \text{ molecule, with} \\ \epsilon_L = 628 \text{ cm}^{-1}. \quad (5)$$

With $I_L = 1000 \text{ W}/\text{cm}^2$ for example, $k_A(\text{SF}_6(\nu_3)) = 1.06 \times 10^5 \text{ s}^{-1}$ and $k_A(\text{UF}_6(\nu_3)) = 8.02 \times 10^4 \text{ s}^{-1}$.

2.2. Spontaneous emission by QF_6 (process 1)

The spontaneous photon emission or ‘‘Einstein’’ rate \mathcal{A}_{se} for a vibrational $\nu_3 = 1 \rightarrow 0$ transition of the photon-active ν_3 vibration of QF_6 can be expressed by (Eerkens, 1973):

$$\mathcal{A}_{se} = (32\pi^3/3) \{e^2/(\hbar c)\} (c \mathfrak{D}_{01}^2/\lambda_3^3) = (8\pi^2/3) (e^2/c) (z_3/\lambda_3)^2/M_3, \quad (6a)$$

or:

$$\mathcal{A}_{se} = 1.220 \times 10^4 \{z_3/\lambda_3 (\mu\text{m})\}^2/M_3 (\text{amu}), \text{ s}^{-1}. \quad (6b)$$

Here \mathfrak{D}_{01}^2 is the dipole-derivative transition matrix for $\nu_3 = 0 \leftrightarrow 1$ transitions, given by:

$$\mathfrak{D}_{01}^2 = \{\hbar/(4\pi c)\} \lambda_3 z_3^2/M_3, \text{ cm}^2. \quad (7)$$

The derivative dipole charge $z_b \equiv (z_b)_{01}$ or derivative dipole moment $(\mu'_b)_{01} = ez_b$, and the vibrational mass M_b of vibration mode b have been calculated for some polyatomic molecules (Kraus, 1967), while emission wavelengths λ_b are usually known from spectral measurements ($\lambda_3 \approx 10.5 \mu\text{m}$ for SF_6 and $\lambda_3 \approx 15.9 \mu\text{m}$ for UF_6). More often $\mathcal{A}_{se}(\nu_b)$ is measured from which values for z_b^2/M_b can be derived. Then with M_b calculated or estimated, z_b can be deduced.

QF_6 molecules have two photon-active vibrations, ν_3 and ν_4 . For SF_6 and UF_6 , values of $\mathcal{A}_{se}[\text{SF}_6(\nu_3)] = 23.8 \text{ s}^{-1}$ and $\mathcal{A}_{se}[\text{UF}_6(\nu_3)] = 12.0 \text{ s}^{-1}$, or $\tau_{se}[\text{SF}_6(\nu_3)] = 0.042 \text{ s}$ and $\tau_{se}[\text{UF}_6(\nu_3)] = 0.083 \text{ s}$ have been measured (Burak *et al.*, 1970; Kim & Person, 1981). This yields $z_3^2/M_3 = 0.215$ for SF_6 and $z_3^2/M_3 = 0.249$ for UF_6 . Using estimated values of $M_3(\text{SF}_6) = 18.77 \text{ amu}$ and $M_3(\text{UF}_6) = 119.88 \text{ amu}$, one deduces that $z_3(\text{SF}_6) = 2.01$ and $z_3(\text{UF}_6) = 5.46$. Lifetimes of other QF_6 molecules for $\nu_3 = 1 \rightarrow \nu_3 = 0$ transitions are of the same magnitude. That is $0.03 < \tau_{se}[\text{QF}_6(\nu_3)] < 0.3 \text{ s}$ generally. Thus with transit times $t_{tr} < 2 \times 10^{-3} \text{ s}$, there is little chance for laser-excited $\text{QF}_6(\nu_3)^*$ monomers to loose vibrational energy by photon emission during its journey in the free jet. If the ν_3 vibration is excited in $\text{QF}_6:\text{G}$ or $\text{QF}_6:\text{QF}_6$ dimers, much faster predissociations prevail over relaxation by spontaneous emission; again few photons are released.

3. COLLISION-INDUCED REACTIONS OF EXCITED AND UNEXCITED QF₆ MOLECULES

3.1. Collision rates, mean free paths; overview of reactive processes

The contact collision rate k_c of QF₆ molecules with molecules M (M = G or QF₆) is:

$$k_c = n_M \sigma_{cQ/M} \bar{u}_{Q/M} \\ = 1.41 \times 10^7 \sigma_{cQ/M} (\text{\AA}^2) p_M (\text{Torr}) / \{ (T(\text{K}) M_{Q/M} (\text{amu}))^{1/2} \}, \text{s}^{-1} \quad (8)$$

where n_M is molecular density (cm^{-3}) of M, $\sigma_{cQ/M} = \pi (r_{oQ} + r_{oM})^2$ is the collision cross-section (\AA^2) for QF₆ + M collisions, and $\bar{u}_{Q/M}$ the relative molecular velocity (cm/s) given by:

$$\bar{u}_{Q/M} = \{ (8/\pi) kT / M_{Q/M} \}^{1/2} \\ = 1.457 \times 10^4 \{ T(\text{K}) / M_{Q/M} (\text{amu}) \}^{1/2}, \text{cm/s}. \quad (9)$$

In Eq (8), $n_M (\text{cm}^{-3}) = 0.97 \times 10^{19} p_M (\text{Torr}) / T(\text{K})$ is assumed, and $M_{Q/M} (\text{amu}) = M_Q M_M / (M_Q + M_M)$, where QF₆ is shortened to Q in subscripts. r_{oQ} , r_{oG} are molecular contact radii of QF₆ and G (Eerkens, 2001a). For SF₆ or UF₆ diluted in 0.01 torr Ar at T = 50 K for example, $k_c(\text{SF}_6/\text{Ar}) = 7.94 \times 10^5 \text{s}^{-1}$ and $k_c(\text{UF}_6/\text{Ar}) = 9.88 \times 10^5 \text{s}^{-1}$. Table 1 lists additional rates k_c for other gases.

The mean collision-free path ℓ_c for a QF₆ molecule diluted in carrier gas G at temperature T is:

$$\ell_c = (n_G \sigma_{cQ/G})^{-1} = 1.04 \times 10^{-3} T(\text{K}) / \{ \sigma_{cQ/G} (\text{\AA}^2) p_G (\text{torr}) \}, \text{cm}, \quad (10)$$

where $\sigma_{cQ/G}$ is the elastic collision cross-section for QF₆ + G encounters and $p_G = (1 - y_Q) p_{\text{tot}}$ is carrier gas pressure. QF₆+QF₆ collisions are neglected since mole fraction $y_Q \ll 1$ is assumed.

Most QF₆ + M encounters result in elastic collisions, but some result in the formation of transient QF₆:M dimers. For vibrationally excited QF₆* molecules, aside from elastic collisions, encounters with M can result in direct VT conversions or in VV transfers if M = QF₆ with probabilities ϕ_{VT} or ϕ_{VV} . Also a dimer QF₆*:M can form with probability $\phi_{df}(Q/M)$, which (pre-)dissociates within microseconds (Smalley *et al.*, 1976; Beswick & Jortner, 1978; Bernstein & Kolb, 1979; Geraedts *et al.*, 1981, 1982; Snells & Reuss, 1987; Liedenbaum *et al.*, 1989; VanBladel & Vander Avoird, 1990; McCaffrey & Marsh, 2002). The outcome of both ϕ_{VT} and ϕ_{df} processes is that epithermal QF₆ and M molecules recoil off each other after conversion of V to T energy, as discussed below. Direct resonant VV transfer between an excited QF₆* and unexcited QF₆ (i.e., M = QF₆) has a high probability but does not effect overall V storage. However while the net energy distribution is not changed by VV transfers, for MLIS processes, near-resonant exchanges ${}^i\text{QF}_6^* + {}^j\text{QF}_6 \rightarrow {}^i\text{QF}_6 + {}^j\text{QF}_6^*$ generate undesirable isotopic losses (isotope scrambling). Such losses are minimized by a high dilution of QF₆ in carrier G.

Table 1A. Molecular parameters for SF₆(ν_3) and UF₆(ν_3) gas-phase collisional VT relaxations

Collision pair QF ₆ */G	Reduced mass $M_{Q/G}$, amu	Collision cross-section σ_c , \AA^2	Repulsive range L_R , \AA	Gas Temperature $T = 200$ K				
				χ_3	$F_C(\chi_3)$	ϕ_{VT3}	k_c/p_G , $\text{s}^{-1}/\text{torr}$	$k_W p_G$, s^{-1} torr
SF ₆ */H ₂	1.97	199.5	0.098	17.9	0.145	2.76×10^{-2}	1.416×10^8	295.80
SF ₆ */He	3.89	180.4	0.108	42.9	3.45×10^{-2}	3.34×10^{-3}	9.116×10^7	232.80
SF ₆ */N ₂	23.5	237.1	0.108	261.4	8.26×10^{-5}	1.32×10^{-6}	4.877×10^7	72.10
SF ₆ */Ar	31.4	223.1	0.126	469.6	3.10×10^{-6}	3.77×10^{-8}	3.970×10^7	66.28
SF ₆ */Xe	69.1	258.3	0.137	1,232	1.92×10^{-9}	1.05×10^{-11}	3.098×10^7	38.59
SF ₆ */UF ₆	103.2	342.2	0.096	907.1	2.75×10^{-8}	1.00×10^{-10}	3.942×10^7	20.31
UF ₆ */H ₂	1.99	221.0	0.107	9.44	0.281	1.623	1.904×10^8	218.26
UF ₆ */He	3.96	201.0	0.117	22.4	0.107	0.311	1.239×10^7	168.68
UF ₆ */N ₂	25.9	260.6	0.117	148.3	9.7×10^{-4}	4.3×10^{-4}	6.122×10^7	52.03
UF ₆ */Ar	35.9	245.9	0.135	270.3	7.0×10^{-5}	2.2×10^{-5}	4.935×10^7	46.61
UF ₆ */Xe	95.6	282.8	0.146	847.9	4.7×10^{-8}	5.7×10^{-9}	3.436×10^7	25.15
UF ₆ */SF ₆	103.2	342.2	0.096	398.1	8.6×10^{-6}	9.6×10^{-7}	3.942×10^7	20.31
UF ₆ */UF ₆	176.0	370.3	0.110	883.1	3.4×10^{-8}	1.1×10^{-9}	3.749×10^7	12.52

Notes: (a) Molecular Masses M_G or M_Q (amu) are: 2 for G = H₂; 4 for G = He; 28 for G = N₂; 40 for G = Ar; 131 for G = Xe; 146 for Q or G = SF₆; 352 for Q or G = UF₆. $R = 1$ cm is assumed to calculate $k_W p_G$. (b) Vibrational constants assumed for the ν_3 vibrations are: for SF₆, $\nu_3 = 948 \text{cm}^{-1}$, $M_3 = 18.77$ amu, $x_3 = 0.0029$; and for UF₆, $\nu_3 = 627.7 \text{cm}^{-1}$, $M_3 = 119.88$ amu, $x_3 = 0.0017$. (c) VV transfer probabilities for ${}^i\text{QF}_6(\nu_3) + {}^j\text{QF}_6 \rightarrow {}^i\text{QF}_6 + {}^j\text{QF}_6(\nu_3)$ exchanges are calculated to be: $\phi_{VV}(\text{SF}_6(\nu_3)) = 1.09 \times 10^{-4}$ and $\phi_{VV}(\text{UF}_6(\nu_3)) = 2.56 \times 10^{-4}$, at $T = 200$ K.

Table 1B. Molecular parameters for SF₆(ν₃) and UF₆(ν₃) gas-phase collisional VT relaxations

Collision pair QF ₆ [*] /G	Gas Temperature T = 100 K					Gas Temperature T = 30 K				
	χ ₃	F _C (χ ₃)	ϕ _{VT3}	k _c /p _G , s ⁻¹ /torr	k _w p _G , s ⁻¹ torr	χ ₃	F _C (χ ₃)	ϕ _{VT3}	k _c /p _G , s ⁻¹ /torr	k _w p _G , s ⁻¹ torr
SF ₆ [*] /H ₂	35.88	4.93 × 10 ⁻²	1.55 × 10 ⁻⁴	2.002 × 10 ⁸	104.58	119.6	2.04 × 10 ⁻³	1.14 × 10 ⁻¹³	3.656 × 10 ⁸	17.20
SF ₆ [*] /He	85.9	6.12 × 10 ⁻³	9.78 × 10 ⁻⁶	1.289 × 10 ⁸	82.31	286.3	5.13 × 10 ⁻⁵	1.45 × 10 ⁻¹⁵	2.353 × 10 ⁸	13.52
SF ₆ [*] /N ₂	522.7	1.58 × 10 ⁻⁶	4.19 × 10 ⁻¹⁰	6.900 × 10 ⁷	25.49	1,742	6.3 × 10 ⁻¹¹	2.94 × 10 ⁻²²	1.259 × 10 ⁸	4.187
SF ₆ [*] /Ar	939.3	2.10 × 10 ⁻⁸	4.09 × 10 ⁻¹²	5.615 × 10 ⁷	23.43	3,131	6.2 × 10 ⁻¹⁴	2.19 × 10 ⁻²⁵	1.025 × 10 ⁸	3.848
SF ₆ [*] /Xe	2,464	1.3 × 10 ⁻¹²	1.14 × 10 ⁻¹⁶	4.381 × 10 ⁷	13.64	8,213	1.6 × 10 ⁻²⁰	2.51 × 10 ⁻³²	7.998 × 10 ⁷	2.243
SF ₆ [*] /UF ₆	1,814	4.1 × 10 ⁻¹¹	2.46 × 10 ⁻¹⁵	5.575 × 10 ⁷	7.18	6,047	3.5 × 10 ⁻¹⁸	3.77 × 10 ⁻³⁰	1.018 × 10 ⁸	1.787
UF ₆ [*] /H ₂	18.9	0.1357	4.09 × 10 ⁻²	2.692 × 10 ⁸	77.17	63.0	1.34 × 10 ⁻²	1.55 × 10 ⁻⁸	4.915 × 10 ⁸	12.67
UF ₆ [*] /He	44.9	3.15 × 10 ⁻²	4.76 × 10 ⁻³	1.752 × 10 ⁸	59.64	150.0	8.99 × 10 ⁻⁴	5.24 × 10 ⁻¹⁰	3.198 × 10 ⁷	9.792
UF ₆ [*] /N ₂	296.5	4.4 × 10 ⁻⁵	1.01 × 10 ⁻⁶	8.659 × 10 ⁷	18.40	998.3	1.34 × 10 ⁻⁸	1.19 × 10 ⁻¹⁵	1.581 × 10 ⁷	3.233
UF ₆ [*] /Ar	540.6	1.3 × 10 ⁻⁶	2.11 × 10 ⁻⁸	6.979 × 10 ⁷	16.48	1,802	4.4 × 10 ⁻¹¹	2.81 × 10 ⁻¹⁸	1.274 × 10 ⁸	2.707
UF ₆ [*] /Xe	1,696	8.3 × 10 ⁻¹¹	5.23 × 10 ⁻¹³	4.859 × 10 ⁷	8.890	5,653	1.1 × 10 ⁻¹⁷	2.59 × 10 ⁻²⁵	8.872 × 10 ⁷	1.402
UF ₆ [*] /SF ₆	796.1	7.8 × 10 ⁻⁷	4.53 × 10 ⁻¹⁰	5.575 × 10 ⁷	7.181	2,154	5.1 × 10 ⁻¹³	1.14 × 10 ⁻²⁰	1.018 × 10 ⁸	1.180
UF ₆ [*] /UF ₆	1,766	4.0 × 10 ⁻¹¹	6.59 × 10 ⁻¹⁴	5.302 × 10 ⁷	4.426	5,887	5.5 × 10 ⁻¹⁸	7.23 × 10 ⁻²⁶	9.680 × 10 ⁷	0.727

Notes: (a) Vibrational constants assumed for the ν₃ vibrations are: for SF₆, ν₃ = 948 cm⁻¹, M₃ = 18.77 amu, x₃ = 0.0029; and for UF₆, ν₃ = 627.7 cm⁻¹, M₃ = 119.88 amu, x₃ = 0.0017. (b) VV transfer probabilities for ⁱQF₆(ν₃) + ^jQF₆ → ⁱQF₆ + ^jQF₆(ν₃) exchanges are calculated to be: ϕ_{VV}(SF₆(ν₃)) = 5.45 × 10⁻⁵ and ϕ_{VV}(UF₆(ν₃)) = 1.28 × 10⁻⁴, at T = 100 K; and ϕ_{VV}(SF₆(ν₃)) = 1.63 × 10⁻⁵ and ϕ_{VV}(UF₆(ν₃)) = 3.84 × 10⁻⁵, at T = 30 K. (c) R = 1 cm is assumed to calculate k_wp_G.

3.2. Direct specular VT relaxations (process 2)

In a gas mixture of QF₆ diluted in carrier gas G, VT deexcitations of QF₆^{*} through contact collisions QF₆^{*} + G → QF₆ + G + K.E. occur at rates:

$$k_{VT} = k_c \phi_{VT}, s^{-1}. \tag{11}$$

Here k_c is given by (8) and VT transition probability ϕ_{VT3} = ϕ_{VT}(QF₆(ν₃)) is (Eerkens, 2001a):

$$\begin{aligned} \phi_{VT3} &= (8kT/\epsilon_3)(M_3/M_{Q/G})\zeta_3^2 F_A F_C \exp(-\frac{1}{2}\epsilon_3/kT) \\ &\approx (2kT/\epsilon_3)(M_3/M_{Q/G})F_C \exp(-\frac{1}{2}\epsilon_3/kT) \end{aligned} \tag{12}$$

with ε₃ = hν₃ and we assume ζ₃²F_A ~ 0.25. The collision function F_C is given by:

$$F_C = F_C(\chi) = (1 + 0.4548\chi^{5/6})(3\chi^{1/3}/2)^2 \operatorname{csch}^2(3\chi^{1/3}/2), \tag{13}$$

with:

$$\chi = \chi_{Q/G} = 0.21 M_{Q/G} L_R^2 \Delta\epsilon/T. \tag{14}$$

In (14), L_R is the repulsive range parameter in Å, Δε = ε₃ equals the energy quantum (in cm⁻¹) that is VT-converted, M_{Q/G} is the reduced mass of the collision partners in amu, and T is the gas temperature in K. For χ > ~20, Eq. (13) reduces to the simpler SSH relation (Eerkens, 2001a; Schwartz *et al.*, 1952; Schwartz & Herzfeld, 1954; Yardley, 1980):

$$F_C(\chi) = 4(\pi/3)^{1/2} \chi^{3/2} \exp(-3\chi^{1/3}) \tag{15}$$

VT deexcitations can also take place in collisions of QF₆^{*} with a like QF₆ molecule, with M_G replaced by M_Q in the above expressions. However in QF₆^{*} + QF₆ encounters, resonant VV transfers (process 3) have a much higher probability of occurring than the VT process 2.

Using molecular parameters listed in Table 1, calculated VT probabilities at different T for SF₆(ν₃)/G and UF₆(ν₃)/G with G = H₂, He, N₂, Ar, Xe, SF₆, and UF₆ are listed in Table 1. They show the enormous effect of mass M_G and T on direct VT probabilities and rates.

3.3. Direct specular resonant VV transfers (process 3)

For a direct VV transfer of ν₃ in a QF₆(ν₃)/QF₆ contact collision, the probability is (Eerkens, 2001a):

$$\phi_{VV3} = \mathfrak{S}_3 \mathfrak{R}_3 = (M_3/M_{Q/Q})(kT/\epsilon_3)x_3, \tag{16}$$

where:

$$\begin{aligned} \mathfrak{S}_3 &\equiv \mathfrak{S}(\text{QF}_6(\nu_3)/\text{QF}_6) \\ &= 16kT(\zeta_3^2/\hbar^2)(M_3^2/M_{Q/Q})F_A F_C \exp(-\frac{1}{2}|\Delta\epsilon|/kT) \\ &\approx 4(kT/\hbar^2)(M_3^2/M_{Q/Q}), \end{aligned} \tag{17}$$

and:

$$\begin{aligned} \mathfrak{R}_3 &\equiv \mathfrak{R}(\text{QF}_6(\nu_3)/\text{QF}_6) = \frac{1}{2}[\hbar^2/(M_3\epsilon_3)]\Omega_{\text{anh}} \\ &= \frac{1}{2}[\hbar^2/(M_3\epsilon_3)][(m!/n!)]x_3^{m-n-1}/(m-n)^2 \\ &= \hbar^2 x_3/(4M_3\epsilon_3). \end{aligned} \tag{18}$$

Here ν_b , x_b , M_b , ζ_b^2 , are the fundamental frequency, anharmonic constant, mass constant, and steric collision factor for internal vibration b in molecule QF_6 (in the present case $b = 3$), while in (17), we assumed $\zeta_3^2 F_A \sim 0.25$ again, and we set $F_C = 1$ since $\Delta\epsilon = 0$ for a VV transfer. For a two-quantum change in a QF_6QF_6 quantum box with $v_3 = 1 \rightarrow 0 \rightarrow 1$, one can as an approximation set $m - n = \Sigma|\Delta v_3| = 2$, with effective values $m = 2$ and $n = 0$ in Ω_{anh} used in Eq. (18). Note also that $M_{\text{Q/Q}} = 0.5 M_{\text{Q}}$. The VV rate in the gas mix is then:

$$\begin{aligned} k_{\text{VV}} &= \tau_{\text{VV}}^{-1} = \phi_{\text{VV}} y_{\text{Q}} (\sigma_{\text{Q/Q}} / \sigma_{\text{Q/G}}) (M_{\text{Q/G}} / M_{\text{Q/Q}})^{1/2} k_{\text{c}} \\ &= \phi_{\text{VV}} y_{\text{Q}} c_{\text{Q/Q}} k_{\text{c}}, \text{ s}^{-1}, \end{aligned} \quad (19)$$

with:

$$\begin{aligned} c_{\text{Q/Q}} &= (\sigma_{\text{Q/Q}} / \sigma_{\text{Q/G}}) (M_{\text{Q/G}} / M_{\text{Q/Q}})^{1/2} \\ &= \{2r_{\text{oQ}} / (r_{\text{oQ}} + r_{\text{oG}})\}^2 \{2M_{\text{G}} / (M_{\text{Q}} + M_{\text{G}})\}^{1/2}. \end{aligned} \quad (20)$$

Here y_{Q} is the mole fraction of QF_6 in the QF_6/G gas mix, and k_{c} is the QF_6/G collision rate given by (8). The factor $c_{\text{Q/Q}}$ corrects for different collision cross-sections and masses of QF_6/QF_6 interactions. Table 4 of (Eerkens, 2001a) lists some values of collision radii r_{oQ} and r_{oG} needed in (20) for molecules QF_6 and G , while the reduced mass $M_{\text{Q/M}} = 2M_{\text{Q}}M_{\text{M}} / (M_{\text{Q}} + M_{\text{M}})$.

Using values for M_3 , ϵ_3 , x_3 , $\sigma_{\text{Q/Q}}$, $M_{\text{Q/Q}}$ from Table 1, one finds from (16) for example at $T = 50$ K, that $\phi_{\text{VV}}(\text{SF}_6(\nu_3)/\text{SF}_6) = 2.52 \times 10^{-5}$ and $\phi_{\text{VV}}(\text{UF}_6(\nu_3)/\text{UF}_6) = 6.40 \times 10^{-5}$. For 2% SF_6 or UF_6 diluted in 10^{-2} torr of Ar, one has from (19) that $\tau_{\text{VV}}(\text{SF}_6(\nu_3)/\text{SF}_6) = 8.2 \times 10^{-3}$ s, and $\tau_{\text{VV}}(\text{UF}_6(\nu_3)/\text{UF}_6) = 2.36 \times 10^{-3}$ s. These times are longer or comparable to t_{tr} and $\tau_{\text{df}} (< 10^{-3}$ s) at $T < 50$ K.

3.4. Dimer formation rates (process 4)

It was shown in (Eerkens, 2001a) that the dimer formation probability ϕ_{df} can be expressed by:

$$\begin{aligned} \phi_{\text{df}} &\approx f_{2\text{Q/M}} i_* \phi_{\text{TV}'}((v_{\text{d}} - 1) \rightarrow v_{\text{d}}) \exp(\eta_*) \\ &= f_{2\text{Q/M}} v_{\text{d}} \phi_{\text{o}} \{1 - (1 + \eta_*) \exp(-\eta_*)\} \end{aligned} \quad (21)$$

where:

$$\eta_* = \epsilon_*/kT = \frac{1}{4} \epsilon_{\alpha}^2 / (D_{\alpha} kT) \quad (22)$$

$$i_* = 1 - (1 + \eta_*) \exp(-\eta_*) \quad (23)$$

$$\begin{aligned} f_{2\text{Q/M}} &= (y_{\text{Q}} M_{\text{Q}} + y_{\text{M}} M_{\text{M}}) \\ &\times (y_{\text{Q}} M_{\text{M}} / M_{\text{Q}} + y_{\text{M}} M_{\text{Q}} / M_{\text{M}}) / \\ &\times (M_{\text{Q}} + M_{\text{M}} + y_{\text{Q}} M_{\text{Q}} + y_{\text{M}} M_{\text{M}}) \end{aligned} \quad (24)$$

$$\phi_{\text{TV}'}((v_{\text{d}} - 1) \rightarrow v_{\text{d}}) = v_{\text{d}} \phi_{\text{o}} \exp(-\eta_*) \quad (25)$$

$$v_{\text{d}} = 2D_{\alpha} / \epsilon_{\alpha} - \frac{1}{2}, \quad (26)$$

$$\phi_{\text{o}} = \phi_1 \exp(-\phi_1) \quad (27)$$

$$\phi_1 \approx 2\rho_{\text{Q/M}} (kT / \epsilon_{\alpha}) \exp(-0.5\eta_*) \quad (28)$$

$$\begin{aligned} \rho_{\text{Q/M}} &= M_{\text{Q/M}} / M_{\text{Q/(Q+M)}} \\ &= M_{\text{M}} (2M_{\text{Q}} + M_{\text{M}}) / (M_{\text{Q}} + M_{\text{M}})^2. \end{aligned} \quad (29)$$

Here v_{d} is the highest (dissociation) vibrational quantum level in the dimer potential well, while M_{Q} , M_{M} , y_{Q} , y_{M} are molecular masses and mole fractions of QF_6 and M ($\text{M} = \text{G}$ or $\text{Q} \equiv \text{QF}_6$). Energy $\epsilon_{\alpha} = h\nu_{\alpha}$ is the fundamental energy (frequency) quantum and D_{α} is the well-depth of the dimer bond. We use V' to designate dimer-bond vibration as opposed to V (without a prime) for internal high-energy molecular vibrations. The dimer formation rate k_{df} is:

$$k_{\text{df}} = k_{\text{c}} \phi_{\text{df}}, \text{ s}^{-1}, \quad (30)$$

with k_{c} given by (8) and ϕ_{df} by (21).

D_{α} values for various collision partners can be obtained from Table 4 in (Eerkens, 2001a), assuming $(D_{\alpha})_{\text{Q/M}} = (D_{\alpha\text{Q}} D_{\alpha\text{M}})^{1/2}$, while ν_{α} can be calculated from Eq. (19) in (Eerkens, 2001a), with values of $r_{\text{o}} = \frac{1}{2}(r_{\text{oQ}} + r_{\text{oM}})$ taken from the same table. For 2% SF_6 or 2% UF_6 diluted in 0.01 torr of H_2 for example, one finds $\phi_{\text{df}}(\text{SF}_6/\text{H}_2) = 5.89 \times 10^{-3}$ and $\phi_{\text{df}}(\text{UF}_6/\text{H}_2) = 4.19 \times 10^{-3}$ at $T = 50$ K. With Ar instead of H_2 , one obtains $\phi_{\text{df}}(\text{SF}_6/\text{Ar}) = 6.31 \times 10^{-4}$, $\phi_{\text{df}}(\text{UF}_6/\text{Ar}) = 5.87 \times 10^{-4}$ at $T = 50$ K. In 0.01 torr of carrier gas, the dimer formation rates are then $k_{\text{df}}(\text{SF}_6/\text{H}_2) = 1.67 \times 10^4 \text{ s}^{-1}$ and $k_{\text{df}}(\text{SF}_6/\text{Ar}) = 501 \text{ s}^{-1}$, while $k_{\text{df}}(\text{UF}_6/\text{H}_2) = 1.59 \times 10^4 \text{ s}^{-1}$ and $k_{\text{df}}(\text{UF}_6/\text{Ar}) = 579 \text{ s}^{-1}$. Other calculated values of ϕ_{df} for selected gas mixtures at various temperatures are listed in Table 2. The table illustrates the diversity of dimerization rates due to the strong effect of mass M_{G} and temperature T in the dimer formation process.

Figures 2 and 3 show plots of ϕ_{VT3} and ϕ_{df} versus gas temperature T for different SF_6/G and UF_6/G gas mixtures. The figures clearly show that towards lower temperatures, dimer formation/predissociation VT conversions are more probable than direct collisional VT relaxations. In some early (1970s) measurements of VT rates, researchers observed that vibrational relaxation rates, after initially dropping as expected, increased again towards lower temperatures (Yardley 1980). Except for light elements, this was in conflict with the collisional VT theory of Schwartz *et al.* (1952) and Schwartz & Herzfeld (1954), and often ascribed to possible VR (Vibration \rightarrow Rotation) transfers, even though collisional VR conversions are rather improbable quantum-mechanically. By including low-temperature two-body dimer

Table 2. Dimerization parameters for SF₆/G and UF₆/G encounters

Dimer pair QF ₆ /G ^(a)	Gas Temperature T = 200 K			Gas Temperature T = 100 K			Gas Temperature T = 30 K					
	Dimer D _e ^(b) , cm ⁻¹	Dimer ε _e ^(c) , cm ⁻¹	ν _d	η _*	φ _{dd}	φ _{df}	η _*	φ _{dd}	φ _{df}	η _*	φ _{dd}	φ _{df}
SF ₆ /H ₂	67.75	58.0	1.829	9.32 × 10 ⁻²	1.85 × 10 ⁻³	1.85 × 10 ⁻³	1.86 × 10 ⁻¹	1.07 × 10 ⁻¹	3.54 × 10 ⁻³	6.22 × 10 ⁻¹	7.50 × 10 ⁻³	1.82 × 10 ⁻²
SF ₆ /He	36.74	32.1	1.792	5.22 × 10 ⁻²	1.05 × 10 ⁻³	1.05 × 10 ⁻³	1.04 × 10 ⁻¹	1.09 × 10 ⁻¹	2.48 × 10 ⁻³	3.48 × 10 ⁻¹	7.32 × 10 ⁻³	6.74 × 10 ⁻²
SF ₆ /N ₂	107.0	19.4	10.51	6.59 × 10 ⁻³	1.07 × 10 ⁻⁵	1.07 × 10 ⁻⁵	1.32 × 10 ⁻²	2.62 × 10 ⁻²	1.76 × 10 ⁻⁴	4.39 × 10 ⁻²	2.50 × 10 ⁻³	1.79 × 10 ⁻³
SF ₆ /Ar	124.6	18.7	12.83	5.24 × 10 ⁻³	2.23 × 10 ⁻⁶	2.23 × 10 ⁻⁶	1.05 × 10 ⁻²	1.96 × 10 ⁻²	7.67 × 10 ⁻⁵	3.49 × 10 ⁻²	1.83 × 10 ⁻³	7.52 × 10 ⁻⁴
SF ₆ /Xe	169.2	13.6	24.29	2.05 × 10 ⁻³	1.09 × 10 ⁻¹⁰	1.09 × 10 ⁻¹⁰	4.11 × 10 ⁻³	7.81 × 10 ⁻³	3.45 × 10 ⁻⁷	1.37 × 10 ⁻²	1.97 × 10 ⁻⁴	7.18 × 10 ⁻⁵
SF ₆ /UF ₆	234.3	11.4	40.54	8.85 × 10 ⁻⁴	1.38 × 10 ⁻¹⁴	1.38 × 10 ⁻¹⁴	2.08 × 10 ⁻³	2.60 × 10 ⁻³	2.69 × 10 ⁻⁹	6.93 × 10 ⁻³	2.17 × 10 ⁻⁵	2.77 × 10 ⁻⁶
UF ₆ /H ₂	88.19	62.8	2.309	8.35 × 10 ⁻²	1.48 × 10 ⁻³	1.48 × 10 ⁻³	9.6 × 10 ⁻²	8.36 × 10 ⁻²	2.76 × 10 ⁻³	5.56 × 10 ⁻¹	5.99 × 10 ⁻³	6.92 × 10 ⁻³
UF ₆ /He	47.83	34.4	2.281	4.61 × 10 ⁻²	8.98 × 10 ⁻⁴	8.98 × 10 ⁻⁴	9.23 × 10 ⁻²	9.81 × 10 ⁻²	1.86 × 10 ⁻³	3.08 × 10 ⁻¹	5.16 × 10 ⁻³	4.07 × 10 ⁻²
UF ₆ /N ₂	139.3	20.1	13.34	5.42 × 10 ⁻³	5.55 × 10 ⁻⁵	5.55 × 10 ⁻⁵	1.09 × 10 ⁻²	1.69 × 10 ⁻²	2.94 × 10 ⁻⁴	3.62 × 10 ⁻²	1.89 × 10 ⁻³	3.89 × 10 ⁻⁴
UF ₆ /Ar	162.2	19.0	16.57	4.15 × 10 ⁻³	2.16 × 10 ⁻⁵	2.16 × 10 ⁻⁵	8.31 × 10 ⁻³	1.16 × 10 ⁻²	1.79 × 10 ⁻⁴	2.77 × 10 ⁻²	1.56 × 10 ⁻³	1.25 × 10 ⁻⁴
UF ₆ /Xe	220.2	12.7	34.31	1.36 × 10 ⁻³	6.08 × 10 ⁻⁹	6.08 × 10 ⁻⁹	2.71 × 10 ⁻³	3.50 × 10 ⁻³	2.18 × 10 ⁻⁶	9.04 × 10 ⁻³	2.66 × 10 ⁻⁴	5.88 × 10 ⁻⁶
UF ₆ /SF ₆	234.3	11.4	40.54	1.04 × 10 ⁻³	7.50 × 10 ⁻¹⁰	7.50 × 10 ⁻¹⁰	2.08 × 10 ⁻³	2.60 × 10 ⁻³	6.62 × 10 ⁻⁷	6.93 × 10 ⁻³	1.57 × 10 ⁻⁴	2.77 × 10 ⁻⁶
UF ₆ /UF ₆	305.0	9.59	63.10	5.63 × 10 ⁻⁴	1.98 × 10 ⁻¹⁴	1.98 × 10 ⁻¹⁴	1.16 × 10 ⁻³	8.00 × 10 ⁻⁴	2.61 × 10 ⁻⁹	3.75 × 10 ⁻³	1.87 × 10 ⁻⁵	8.16 × 10 ⁻⁸

Note: ^a A 2% QF₆-98% G gas mixture is assumed. ^b For heterodimers, D_{eQ/G} = (D_{eQ}D_{eG})^{1/2} where D_{eQ} ≡ D_{eQ/O} and D_{eG} ≡ D_{eG/G} (cm⁻¹) = {39.56/r_{QO/G}(Å)}{D_{eQ/G}(cm⁻¹)/M_{Q/G}(amu)}^{1/2}, with r_{Q/G} = ½(r_{QO} + r_{OG}) and M_{Q/G} = M_QM_G/(M_Q + M_G). Values of D_{eQ/G} ≡ D_{eQ} and r_{OG/G} ≡ r_{OG} are listed in Table 4 of (Eerckens, 2001a).

formation and pre-dissociation of V-excited species, agreement between theory and experiment is restored.

3.5. Collisional dissociation rates of dimers (process 5)

At monomer partial pressures p_Q = y_Qp_{tot} with p_Q less than the homogeneous cluster nucleation pressure p_d (see Section 7.2), the dissociation rate of dimers is (Eerckens, 2001a):

$$k_{dd} = k_{cd} \phi_{dd} = k_c a_d \phi_{dd}, \text{ s}^{-1} \tag{31}$$

with:

$$\phi_{dd} = \frac{1}{2} \{ \exp(-D_\alpha/kT) \{ 1 - \exp(-\epsilon_\alpha/kT) \} \} \tag{32}$$

$$a_d = (\sigma_{cQ/G} M_{Q/G}^{1/2}) / (\sigma_{cQ/G} M_{Q/G}^{1/2}) \approx \{ (r_{oQ} + 2r_{oG}) / (r_{oQ} + r_{oG}) \}^2 \{ 1 + M_G^2 / (M_Q^2 + 2M_Q M_G) \}^{1/2}. \tag{33}$$

Here φ_{dd} is the probability that a dimer QF₆:G dissociates to QF₆ + G in a collision with molecule G. The parameter a_d corrects the collision rate k_c for QF₆/G monomer collisions to the rate k_{cd} = a_dk_c for QF₆:G/G dimer collisions which has a larger collision cross-section and higher reduced mass. Contact radii r_{oQ}, r_{oG}, and reduced masses M_{Q/M} in (33) were discussed in Sections 3.3 and 3.4. Calculated values of φ_{dd} are listed in Table 2. At T ~ 50 K and p_G ~ 0.01 torr for example, Tables 1 and 2 show that 10⁴ < k_{dd} < 10⁵ s⁻¹, or 10⁻⁵ < τ_{dd} < 10⁻⁴ s. This compares with transit times of 10⁻⁵ < t_{tr} < 2 × 10⁻³ s.

4. MOLECULAR MIGRATIONS AND THERMALIZATION OF EPITHERMALS

4.1. Isotope harvesting from laser-irradiated free jets

In isotope separation techniques that utilize laser irradiated free jets of supersonically cooled gas mixtures, advantage is taken of the fact that QF₆:G dimers, QF₆^(*) monomers, and QF₆[!] epithermals, migrate at different rates due to different collision cross-sections and average molecular speeds. After isotope-selective excitation of ⁱQF₆, the ⁱQF₆^{*} will dimerize briefly as ⁱQF₆^{*}:G which rapidly dissociates with VT conversion, creating above-thermal or “epi-thermal” ⁱQF₆[!]. We label epithermal ⁱQF₆[!] with superscript [!] to distinguish them from internal vibrationally excited ⁱQF₆^{*} molecules marked by superscript ^{*} which move at thermal speeds. At low temperatures, under continuous laser pumping, the ⁱQF₆ are distributed over ⁱQF₆^{*}, ⁱQF₆[!], ⁱQF₆:G, and non-excited ⁱQF₆ populations, while ^jQF₆ populate ^jQF₆:G dimer and ^jQF₆ monomer groups. Because of the different population fractions and different migration rates, isotopomers ⁱQF₆ flee

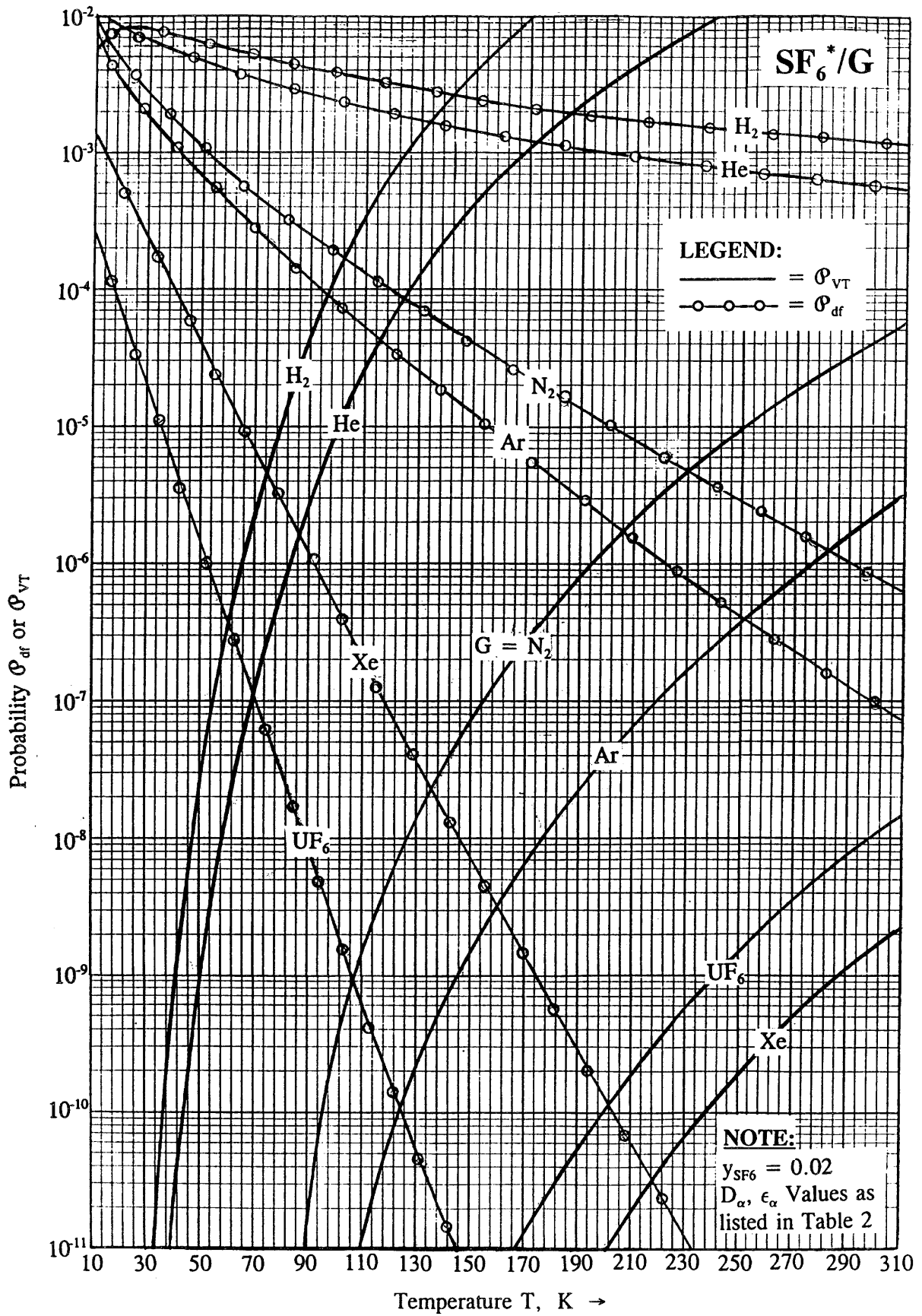


Fig. 2. VT conversion probabilities ϕ_{VT} and ϕ_{df} for SF₆(ν_3)/G gas mixtures.

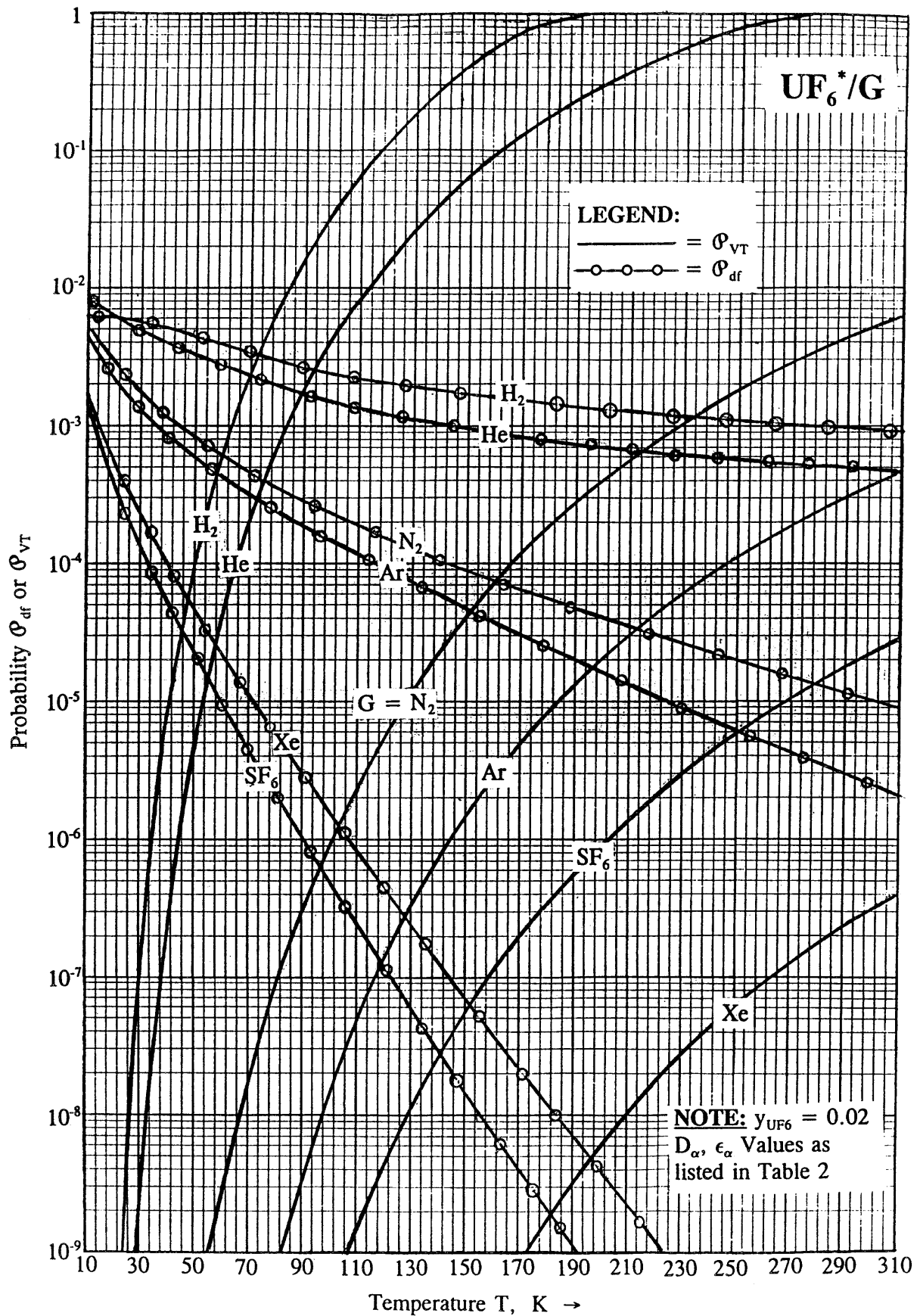


Fig. 3. VT conversion probabilities ϕ_{VT} and ϕ_{df} for $UF_6^*(\nu_3)/G$ gas mixtures.

the jet core at higher rates than the ${}^j\text{QF}_6$, resulting in isotope separation. To summarize, the jet contains ${}^i\text{QF}_6$ of four types, ${}^i\text{QF}_6^*$, ${}^i\text{QF}_6^!$, ${}^i\text{QF}_6$, and ${}^i\text{QF}_6\text{:G}$, which have three different average transport constants, while the ${}^j\text{QF}_6$ are divided over two classes, thermal monomers ${}^j\text{QF}_6$ and slower moving dimers ${}^j\text{QF}_6\text{:G}$, each with different transport parameters (see below).

The peripheral or “rim” gases are pumped out separately from the supersonic jet core gases which exit through a skimmer at the end of the jet chamber (see Fig. 1). As they migrate through the jet core while in transit to the skimmer, laser-excited ${}^i\text{QF}_6$ cycle repeatedly through excitation \rightarrow dimerization \rightarrow dissociation \rightarrow VT-conversion/epithermalization \rightarrow re-thermalization. If ${}^i\text{QF}_6\text{:G}$ dimers are laser-excited instead of ${}^i\text{QF}_6$, the sequence is the same except it starts with dimerization \rightarrow excitation \rightarrow dissociation. . . . Non-excited ${}^j\text{QF}_6$ isotopomers experience only collisional dimerizations and dissociations, but at low temperatures most travel as ${}^j\text{QF}_6\text{:G}$ dimers which migrate more slowly than ${}^i\text{QF}_6$ monomers. Thus ${}^i\text{QF}_6$ escape at higher rates from the jet core than ${}^j\text{QF}_6$, thereby enriching the rim gases with ${}^i\text{QF}_6$.

The mean free path between collisions of a QF_6 molecule diluted in gas G was given by Eq. (10). Table 3 lists $p_G\ell_c$ values for several gases G at different temperatures. For example, at $p_G = 0.01$ torr, $T = 50$ K, and $G = \text{Ar}$, a SF_6 molecule experiences one collision in every 0.22 mm of travel. Thus although “thin,” the gas in a jet with 10 mm radius, still follows Maxwell-Boltzmann kinetics and obeys the diffusion laws, as assumed in what follows.

4.2. Radial molecular migrations and jet core escapes

To estimate the radial outward diffusion of QF_6 molecules and $\text{QF}_6\text{:G}$ dimers from a supersonic free jet, we approximate the actual jet contour by an equivalent cylinder with radius R equal to the skimmer entrance radius (see Section 7). All molecules in the cylinder striking the “wall” at R are then assumed to leave the cylinder, as if the wall were a total molecular absorber. The non-excited and vibrationally excited monomers will be shown to escape the jet at thermal rates k_W , while epithermals escape at rates k_{W1} and dimers leave the jet with a rate constant k_{Wd} , such that $k_{W1} > k_W > k_{Wd} \text{ s}^{-1}$ per molecule.

In (Eerkens, 2001b) it was shown that a batch of N QF_6 molecules diffusing through carrier gas G in a long cylinder with volume $\pi R^2 L$ and surface $2\pi RL$, strike the wall at rates:

$$k_W = \frac{1}{3}(2.405)^2 \bar{u}_{\text{Q/G}} \ell_c / R^2 = 1.928 (\ell_c / R)^2 k_c \\ = 29.3 T^{3/2} / (p_G R^2 \sigma_{\text{cQ/G}} M_{\text{Q/G}}^{1/2}), \text{ s}^{-1} / \text{molecule}, \quad (34)$$

if the wall is 100% absorbing. Here ℓ_c is the mean-free-path and R is cylinder radius in cm, $\sigma_{\text{cQ/G}}$ is the Q/G collision

Table 3. Thermalization parameters for epithermal $\text{SF}_6^!$ and $\text{UF}_6^!$ molecules

Gas Mix $\text{QF}_6^!/\text{G}$	ξ	VT Event $\epsilon_Q, \text{K}^{(1)}$	Coll'n Cr Sec $\sigma_c, \text{\AA}^2$	Gas Temp $T = 200$ K			Gas Temp $T = 100$ K			Gas Temp $T = 30$ K		
				N_T	$\ell_c p_G$ mm torr	$\bar{s}_{th} p_G$ mm torr	N_T	$\ell_c p_G$ mm torr	$\bar{s}_{th} p_G$ mm torr	N_T	$\ell_c p_G$ mm torr	$\bar{s}_{th} p_G$ mm torr
$\text{SF}_6^!/\text{H}_2$	0.0272	18.43	199.5	3.248	0.0104	0.0265	6.232	0.0052	0.0184	17.644	0.00156	0.00926
$\text{SF}_6^!/\text{He}$	0.0538	36.38	180.5	3.106	0.0115	0.0286	5.766	0.0058	0.0195	14.759	0.00173	0.00937
$\text{SF}_6^!/\text{N}_2$	0.3386	219.5	237.2	2.188	0.00877	0.0183	3.431	0.0044	0.0115	6.256	0.00132	0.00464
$\text{SF}_6^!/\text{Ar}$	0.4591	293.3	223.3	1.967	0.00932	0.0184	2.983	0.0047	0.0114	5.179	0.00140	0.00449
$\text{SF}_6^!/\text{Xe}$	0.9834	645.9	258.2	1.466	0.0081	0.0137	2.043	0.0040	0.0081	3.167	0.00121	0.00303
$\text{SF}_6^!/\text{SF}_6$	1.0000	682.1	315.4	1.484	0.0066	0.0113	2.057	0.0033	0.0067	3.167	0.00099	0.00248
$\text{UF}_6^!/\text{H}_2$	0.0113	5.103	269.3	2.227	0.0094	0.0198	4.399	0.0047	0.0139	13.883	0.00141	0.00742
$\text{UF}_6^!/\text{He}$	0.0226	10.15	247.1	2.196	0.01035	0.0216	4.287	0.00518	0.0151	12.924	0.00155	0.00787
$\text{UF}_6^!/\text{N}_2$	0.1510	66.56	312.9	1.904	0.00798	0.0155	3.380	0.00399	0.0103	7.7450	0.00120	0.00470
$\text{UF}_6^!/\text{Ar}$	0.2110	92.17	296.8	1.797	0.00846	0.0160	3.098	0.00423	0.01049	6.658	0.00127	0.00462
$\text{UF}_6^!/\text{Xe}$	0.5870	245.4	336.9	1.364	0.00736	0.01211	2.112	0.00368	0.00754	3.778	0.00110	0.00302
$\text{UF}_6^!/\text{SF}_6$	0.6356	264.8	401.9	1.327	0.00608	0.00987	2.037	0.00304	0.00612	3.596	0.00091	0.00244
$\text{UF}_6^!/\text{UF}_6$	1.0000	451.6	498.8	1.181	0.00562	0.00861	1.708	0.00281	0.00518	2.776	0.00084	0.00198

Note: ¹⁾ Energy quanta released by the ν_3 vibrations are $\epsilon_3 = 948 \text{ cm}^{-1} = 1364 \text{ K}$ for SF_6 , and $\epsilon_3 = 627.7 \text{ cm}^{-1} = 903.3 \text{ K}$ for UF_6 .

cross-section in Å², p_G is in torr, T is in K, and $M_{Q/G} = M_Q M_G / (M_Q + M_G)$ is reduced mass in amu. These units will be used in all final expressions that follow. Table 1 lists typical values of $k_w p_G$. The inverse rate k_w^{-1} equals the average time τ_w for a QF₆ molecule in the cylinder to reach the wall, provided it is not terminated in the gas phase.

In our mathematical model, the “wall absorption” rate equals the jet core escape rate of QF₆ molecules. Because the jet moves at supersonic speed, molecules who cross the “wall” at radius R , can not return to the jet core and can be considered “absorbed” by the “peripheral” or “background” gases in the jet chamber. For a batch of QF₆ molecules entering the jet chamber, which loses QF₆ to the “wall” by radial diffusion as it moves towards the skimmer, the number left in the jet core as a function of time is:

$$N_Q(t) = N_{Q_0} \exp(-k_w t), \text{ QF}_6 \text{ molecules,} \quad (35)$$

Here N_{Q_0} is the tagged QF₆ population entering the jet chamber at $t = 0$. After travel time $t = t_{tr}$, the number of QF₆ molecules remaining in the jet core is:

$$N_Q(t = t_{tr}) = N_{Q_0} \exp(-k_w t_{tr}), \text{ QF}_6 \text{ molecules,} \quad (36)$$

and the number $N_{Q_{esc}}$ or fraction Θ that escaped equals:

$$\Theta = N_{Q_{esc}}(t = t_{tr}) / N_{Q_0} = 1 - \exp(-k_w t_{tr}). \quad (37)$$

Here the transit time $t = t_{tr} = L / \bar{U}$, where L is the travel distance and \bar{U} the average bulk velocity during the jet’s travel through the irradiation chamber.

For a batch of outward diffusing epithermal molecules QF₆¹, the migration rate is similar to thermals, except transport parameters must be adjusted and thermalization must be considered. Using subscript 1 to label epithermal transport parameters, the epithermal migration rate k_{w1} is:

$$\begin{aligned} k_{w1} &= \frac{1}{3} (2.405)^2 \bar{u}_1 \ell_c / R^2 \\ &= 29.3 T_1^{1/2} T / (p_G R^2 \sigma_{cQ/G} M_{Q/G}^{1/2}), \text{ s}^{-1} \text{ per molecule.} \end{aligned} \quad (38)$$

Here we used (34) and replaced $T^{3/2}$ by $T_1^{1/2} T$ since the epithermal velocity \bar{u}_1 is proportional to $T_1^{1/2}$. The mean free path ℓ_c due to scattering of QF₆¹ monomers by molecules G is virtually the same as for thermals and is proportional to T/p_G , if QF₆ is highly diluted in the QF₆/G gas mix.

The average epithermal temperature $\langle T_1 \rangle$ during slow-down can be approximated by the logarithmic mean between the initial kinetic energy ϵ_0 and the final one ϵ_T , that is:

$$\begin{aligned} \langle T_1 \rangle / T &= \mu_1^2 = \epsilon_T^{-1} (\epsilon_0 - \epsilon_T) / \ln(\epsilon_0 / \epsilon_T) \\ &= (\epsilon_Q / \epsilon_T) / \ln(1 + \epsilon_Q / \epsilon_T) \\ &= (\eta_{Q/G} \epsilon_a / \epsilon_T) / \ln(1 + \eta_{Q/G} \epsilon_a / \epsilon_T) \end{aligned} \quad (39)$$

with:

$$\mu_1 = \{(\eta_{Q/G} \epsilon_a / \epsilon_T) / \ln(1 + \eta_{Q/G} \epsilon_a / \epsilon_T)\}^{1/2} = \{a / \ln(1 + a)\}^{1/2}, \quad (40)$$

Here a is defined as:

$$a = \epsilon_Q / \epsilon_T = \eta_{Q/G} \epsilon_a / \epsilon_T, \quad (41)$$

in which ϵ_Q is the original kinetic recoil energy given to QF₆ in the VT conversion by dimer predissociation, ϵ_a is the released quantum of vibrational energy, and $\epsilon_T = kT$ is the thermal kinetic energy. From momentum and energy conservation of dissociating dimer partners one deduces that:

$$\eta_{Q/G} = \epsilon_Q / \epsilon_a = M_G / (M_G + M_Q). \quad (42)$$

The original kinetic energy ϵ_0 of a VT-energized QF₆¹ molecule then equals:

$$\epsilon_0 = \epsilon_Q + \epsilon_T = (1 + a) \epsilon_T. \quad (43)$$

In the case of laser excitation of ν_3 in QF₆ molecules, the quantum energy $\epsilon_a = \epsilon_3 = h\nu_3$.

Note from (42) that the heavier the dimer partner G is, the larger the fraction of the vibrational energy ϵ_a imparted to a recoiling QF₆ molecule. Most useful carrier gases have masses M_G that are less than those of SF₆ ($M_Q = 146$ amu) and UF₆ ($M_Q = 352$ amu). Thus for QF₆ molecules one usually has $\eta_{Q/G} \leq 0.5$. Heavy particles or solid surfaces might look attractive for maximizing ϵ_Q , but one finds that other problems are introduced. Laser isotope separations utilizing cold surfaces are discussed in a separate paper (Eerkens, 2005).

Returning to (38), the “wall” escape rate for epithermals is:

$$\begin{aligned} k_{w1} &= \mu_1 k_w = 1.928 \mu_1 (\ell_c / R)^2 k_c \\ &= 29.3 \mu_1 T^{3/2} / (p_G R^2 \sigma_{cQ/G} M_{Q/G}^{1/2}), \text{ s}^{-1} / \text{molecule,} \end{aligned} \quad (44)$$

and the epithermal escape fraction Θ_1 is:

$$\Theta_1 = 1 - \exp(-\mu_1 k_w t_{tr}). \quad (45)$$

For dimers which move thermally, the collision cross-section and reduced mass is higher than for monomers. That is in (34), one must replace $\sigma_{cQ/G}$ and $M_{Q/G}$ by $\sigma_{cQG/G}$ and $M_{QG/G}$. Using subscripts d for dimers, the escape rate k_{wd} for dimers then equals:

$$\begin{aligned} k_{wd} &= \psi_d k_w = 1.928 (\ell_c / R)^2 \psi_d k_c \\ &= 29.3 T^{3/2} / (p_G R^2 \sigma_{cQG/G} M_{QG/G}^{1/2}), \text{ s}^{-1} \text{ per molecule,} \end{aligned} \quad (46)$$

$$\begin{aligned}\psi_d &= (\sigma_{cQ/G} M_{Q/G}^{1/2}) / (\sigma_{cQG/G} M_{QG/G}^{1/2}) \\ &= \{(r_{oQ} + r_{oG}) / (r_{oQ} + 2r_{oG})\}^2 / \{1 + M_G^2 / (M_Q^2 + 2M_Q M_G)\}^{1/2}.\end{aligned}\quad (47)$$

Here ψ_d , which is less than unity, is the migration rate correction factor for dimers compared to monomers. The QF₆/G collision rate k_c and mean-free-path ℓ_c were given by (8) and (10). The dimer escape fraction is finally:

$$\Theta_d = 1 - \exp(-\psi_d k_w t_{tr}). \quad (48)$$

4.3. Slowing-down parameters for epithermal molecules

The average number of collisions that an epithermal molecule experiences till it is thermalized, and the average distance it moves, can be obtained from ‘‘Fermi Age Theory’’ originally developed for epithermal neutrons instead of molecules (Glasstone & Edlund, 1952). This theory shows that the average number of collisions N_T to thermalize an epithermal molecule equals:

$$\begin{aligned}N_T &= \{\ell_n(\epsilon_0/\epsilon_T)\} / \{\ell_n(\epsilon_{II}/\epsilon_I)\} = \xi^{-1} \ell_n(\epsilon_0/\epsilon_T) \\ &= \xi^{-1} \ell_n(1 + \epsilon_Q/\epsilon_T) = \xi^{-1} \ell_n(1 + a).\end{aligned}\quad (49)$$

Here ϵ_I , ϵ_{II} are kinetic energies of an epithermal molecule before and after a momentum-transfer collision, and the average logarithmic energy decrement ξ equals:

$$\xi = \langle \ell_n(\epsilon_{II}/\epsilon_I) \rangle = 1 + \{\alpha / (1 - \alpha)\} \ell_n(\alpha), \quad (50)$$

with:

$$\alpha = \{(M_Q - M_G) / (M_Q + M_G)\}^2. \quad (51)$$

Kinetic energy ϵ_Q was given by (42), and the ratio $a = \epsilon_Q/\epsilon_T$ by Eq. (41). In Fermi age theory, an epithermal neutron or molecule is considered thermalized when its kinetic energy has dropped to $\epsilon_T = kT$, rather than $(3/2)kT$ (Glasstone & Edlund, 1952). The average fractional energy loss for each epithermal QF₆[†] + G momentum transfer collision is given by:

$$\varpi = 1 - \langle \epsilon_{II}/\epsilon_I \rangle = 1 - (\alpha + 1)/2. \quad (52)$$

If energy losses of QF₆[†] during thermalization are purely due to scattering and momentum transfers, the slowing-down length or migration distance ‘‘as the crow flies,’’ is (Glasstone & Edlund, 1952):

$$\bar{s}_{th} = (6\vartheta_T)^{1/2} = 1.41 N_T^{1/2} \ell_c \quad (53)$$

where ℓ_c and N_T were given by (10) and (49), and the thermalization ‘‘age’’ ϑ_T equals:

$$\vartheta_T = \vartheta_{\epsilon_0 \rightarrow \epsilon_T} \{ (D\ell_c) / (\xi\epsilon) \} d\epsilon = (1/3 \ell_c^2 / \xi) \ell_n(\epsilon_0/\epsilon_T) = \frac{1}{3} \ell_c^2 N_T. \quad (54)$$

Here we assumed $D\ell_c/\xi$ to be independent of energy and the ‘‘flux diffusion coefficient’’ is approximated by $D \approx \frac{1}{3} \ell_c$. Table 3 lists ξ , ϵ_Q , N_T , ℓ_c , and \bar{s}_{th} of SF₆ and UF₆, with various carrier gases at several temperatures T and kinetic energies ϵ_0 .

The thermalization rate of epithermals in the gas (= a feed term for the thermal group), is:

$$\begin{aligned}k_{th} &= \bar{n}_1 / (\ell_c N_T) = \mu_1 k_c / N_T \\ &= 1.41 \times 10^7 (\mu_1 / N_T) p_G \sigma_{cQ/G} / (TM_{Q/G})^{1/2}, \text{ s}^{-1},\end{aligned}\quad (55)$$

where units are in torr, Å², K, and amu, as before. This rate is high and forces epithermal molecules to re-enter the thermal monomer group repeatedly and be re-excited, etc, several times before reaching the wall. The same is true for dimers which are continuously formed and dissociated in collisions. That is, in a unit volume of gas, rapid exchanges take place between populations of the four migrating groups, but under steady-state conditions, the fractional populations are constant (see Section 5). Individual molecules are continuously cycled through laser-excitation, dimerization/predissociation/epithermalization, and re-thermalization in tens of microseconds as they migrate to the wall. However as long as the population fractions for each migrant class are constant, the effective escape rate per molecule per second is k_w for the thermal group, k_{w1} for the epithermal fraction, and k_{wd} for those in the dimer state, even though individual molecules are continuously exchanged between these different migrant groups. That is, under continuous laser pumping, all thermalizing ⁱQF₆ leaving the epithermal group are replaced by newly excited ⁱQF₆^{*} that dimerize, and epithermalize. Thus as long as molecules are not permanently removed in the gas and populations are steady, the migration of ⁱQF₆ can be considered taking place by three independently moving species: a fraction f_{it} at rate k_w for excited or unexcited thermal monomers; a fraction f_{i1} for epithermals at rate k_{w1} ; and a fraction f_{id} at rate k_{wd} for dimers. Steady-state fractional populations $f_{it} = f_{i^*} + f_{im}$, f_{i^*} , f_{i1} , f_{im} , f_{id} of excited, epithermal, and non-excited ⁱQF₆ monomers and dimers are considered next.

5. POPULATION OF DIMERS, LASER-EXCITED MOLECULES, AND EPITHERMALS

5.1. Monomer laser excitation

As mentioned, under steady monomer laser-irradiation, the ⁱQF₆ population is distributed over four distinct groups:

excited species (*), epithermals (!), non-excited monomer molecules (m), and non-excited dimers (d). The fraction f_{i^*} of laser-excited ${}^i\text{QF}_6^*$ is defined as $f_{i^*} = n_{i^*}/n_i = [{}^i\text{QF}_6^*]/[{}^i\text{QF}_6]$, where the brackets (by convention) indicate concentrations. Here $n_i \equiv n_{\text{Qi}}$ is the density (molecules/cm³) of a selected isotopomer ${}^i\text{QF}_6$, $n_Q = \sum_j n_{\text{Qj}}$ is the total density of all QF_6 , while the isotopic abundance of ${}^i\text{QF}_6$ equals $x_i = n_i/n_Q$. Other populations of interest are the fraction $f_{i!}$ of epithermal ${}^i\text{QF}_6^!$ molecules, the fraction f_{im} of non-excited ${}^i\text{QF}_6$ monomers, and fraction f_{id} of non-excited dimers. We shall assume that most dimers formed in the gas mixture will be heterodimers $\text{QF}_6 \cdot \text{G}$ if mole fraction $y_Q < \sim 0.05$. That is, we neglect homo-dimers $\text{QF}_6 \cdot \text{QF}_6$ and trimers, tetramers, etc. Neglect of oligomers other than dimers is reasonable because of the short residence time of the jet in the chamber (Sec. 7.2). A material balance then gives:

$$f_{i^*} + f_{i!} + f_{\text{im}} + f_{\text{id}} = 1. \tag{56}$$

Neglecting excitations of in-flight epithermals and second-step excitations of once-excited species, the excited species production rate under laser irradiation is given by the product $\varphi_L \sigma_A f_{\text{im}} n_i = k_A f_{\text{im}} n_i$, where φ_L is the laser flux, σ_A is the photon absorption cross-section, and $f_{\text{im}} n_i$ is the non-excited monomer population of ${}^i\text{QF}_6$. Then, since $f_{\text{im}} = 1 - f_{i!} - f_{i^*} - f_{\text{id}}$, one has:

$$d(f_{i^*} n_i)/dt = (1 - f_{i^*} - f_{i!} - f_{\text{id}}) n_i k_A - f_{i^*} n_i \{ (1 - e_*) (k_{\text{df}} + k_{\text{v}} + \mathcal{A}_{\text{se}}) + e_* k_{\text{w}} \}, \text{ s}^{-1} \text{ cm}^{-3}. \tag{57}$$

The first term on the right-hand-side of the kinetics balance (57) is the laser excitation rate per unit volume of ${}^i\text{QF}_6$ monomers which produces ${}^i\text{QF}_6^*$, while the second term represents losses of vibrational excited ${}^i\text{QF}_6^*$ due to dimerizations/predissociations and direct VT and VV transfers, spontaneous emissions, and “wall” escapes of ${}^i\text{QF}_6^*$. To-the-wall survival probabilities e_* for QF_6^* in the gas phase are included in (57) to balance all sources and sinks:

$$e_* = \exp\{-(k_{\text{df}} + k_{\text{VV}} + k_{\text{VT}} + \mathcal{A}_{\text{se}}) \tau_{\text{w}}\} = \exp[-0.519(\ell_c/R)^2(\varphi_{\text{df}} + \varphi_{\text{VT}} + \varphi_{\text{VV}} + \mathcal{A}_{\text{se}}/k_c)], \text{ s}^{-1}. \tag{58}$$

Here the average travel time to the wall $\tau_{\text{w}} = k_{\text{w}}^{-1}$. Unless the gas is very thin, $e_* \sim 0$ usually. Parameters k_{df} , k_{w} , and \mathcal{A}_{se} were already reviewed, while k_A was discussed in Section 2.1.

The loss rate $k_{\text{v}} = k_{\text{VV}} + k_{\text{VT}}$ from direct VT and VV transfers of the ν_3 vibration in SF_6^* and UF_6^* equals:

$$k_{\text{v}} = k_{\text{VT3}} + k_{\text{VV3}} = k_c \{ \varphi_{\text{VT3}} + y_Q (1 - x_i) c_{\text{Q/Q}} \varphi_{\text{VV3}} \}, \text{ s}^{-1} \tag{59}$$

Here the collisional encounter rate k_c was given by Eq. (8), φ_{VT3} by (12), φ_{VV3} by (16), and $c_{\text{Q/Q}}$ by (20). At enrichment-favoring temperatures $T \sim 30$ K, and with $p_G \sim 0.01$ torr, $y_Q = 0.02$, and masses $M_G > \sim 10$ amu, Table 1 shows that $\varphi_{\text{VT3}} < \sim 10^{-10}$ and $\varphi_{\text{VV3}} \sim 10^{-4}$, while Table 2 gives $\varphi_{\text{df}} \sim 10^{-3}$. Both φ_{VT} and φ_{VV} decrease with decreasing T , but φ_{df} increases with decreasing T . Under these conditions, with $k_c \sim 10^6 \text{ s}^{-1}$, one obtains $k_{\text{df}} \sim 10^3 \text{ s}^{-1}$, $k_{\text{VT3}} \sim 10^{-4} \text{ s}^{-1}$, $k_{\text{VV3}} \sim 10^2 \text{ s}^{-1}$, while $\mathcal{A}_{\text{se}} \sim 20 \text{ s}^{-1}$. Thus (57) and (58) can be simplified to:

$$d(f_{i^*} n_i)/dt \approx (1 - f_{i^*} - f_{i!} - f_{\text{id}}) n_i k_A - f_{i^*} n_i \{ (1 - e_*) k_{\text{df}} + e_* k_{\text{w}} \}, \text{ s}^{-1} \text{ cm}^{-3}, \tag{60}$$

and:

$$e_* \approx \exp(-k_{\text{df}} \tau_{\text{w}}) = \exp\{-0.519(R/\ell_c)^2 \varphi_{\text{df}}\}, \text{ s}^{-1}. \tag{61}$$

The epithermal population $f_{i!} n_i$ is balanced by the relation:

$$d(f_{i!} n_i)/dt = (1 - e_*) (k_{\text{df}} + k_{\text{VT}}) f_{i^*} n_i - \{ (1 - e_1) k_{\text{th}} + e_1 k_{\text{w1}} \} f_{i!} n_i \approx k_{\text{df}} f_{i^*} n_i - \{ k_{\text{th}} + k_{\text{w1}} e_1 \} f_{i!} n_i. \tag{62}$$

Here k_{df} was given by (30), k_{th} by (55), and k_{w1} by (44). Since for $T < 50$ K, $k_{\text{VT}} \ll k_{\text{df}}$, and usually $e_* \ll 1$, $e_1 \ll 1$, the approximation in (62) applies under enrichment-favoring conditions. The to-the-wall survival probability e_1 for gas-phase epithermals in (62) equals:

$$e_1 = \exp(-k_{\text{th}} \tau_{\text{w1}}) = \exp(-k_{\text{th}}/k_{\text{w1}}) = \exp\{-0.519(R/\ell_c)^2/N_T\}. \tag{63}$$

Here $\mu_1 k_c$ cancels out in the ratio $k_{\text{th}}/k_{\text{w1}}$ in the exponential of (63). Factors e_1 and e_* apply to “leaks” from internal microscopic processes per unit volume in the jet, insuring correct values for f_{i^*} when $R < \ell_c$. Survival factors e_* and e_1 must not be confused with bulk losses Θ or Θ_1 .

The population of non-excited dimers f_{id} is determined finally by the kinetic balance:

$$d(f_{\text{id}} n_i)/dt = f_{\text{im}} n_i k_{\text{df}} - f_{\text{id}} n_i k_{\text{dd}} = (1 - f_{i^*} - f_{i!} - f_{\text{id}}) n_i k_{\text{df}} - f_{\text{id}} n_i k_{\text{dd}} = (1 - f_{i^*} - f_{i!}) n_i k_{\text{df}} - f_{\text{id}} n_i (k_{\text{df}} + k_{\text{dd}}). \tag{64}$$

Under steady-state laser-irradiation and gas flow, $d(f_{i^*} n_i)/dt = d(f_{i!} n_i)/dt = d(f_{\text{id}} n_i)/dt = 0$. Then ignoring k_{VT} since $k_{\text{VT}} \ll k_{\text{df}}$, Eqs (62) and (64) yield:

$$f_{i!} = [(1 - e_*) (k_{df} + k_{VT}) / \{(1 - e_1) k_{th} + e_1 k_{w1}\}] f_{i^*} = \kappa_1 f_{i^*}, \quad (65)$$

with:

$$\begin{aligned} \kappa_1 &= (1 - e_*) (k_{df} + k_{VT}) / \{(1 - e_1) k_{th} + e_1 k_{w1}\} \\ &\approx (1 - e_*) k_{df} / \{(1 - e_1) k_{th}\} \approx k_{df} / k_{th}, \end{aligned} \quad (66)$$

and:

$$f_{id} = (1 - f_{i^*} - f_{i!}) \{k_{df} / (k_{df} + k_{dd})\} = \{1 - (\kappa_1 + 1) f_{i^*}\} \omega_d \quad (67)$$

with:

$$\omega_d = k_{df} / (k_{df} + k_{dd}) = \varphi_{df} / (\varphi_{df} + a_d \varphi_{dd}). \quad (68)$$

Finally, setting (57) equal to 0 and inserting (65) and (67) yields:

$$\begin{aligned} f_{i^*} &= \{(1 - \omega_d) k_A\} / \{(\kappa_1 + 1)(1 - \omega_d) k_A \\ &\quad + (1 - e_*) (k_{df} + k_{VV} + k_{VT} + \mathcal{A}_{se}) + e_* k_W\} \\ &\approx \{(1 - \omega_d) k_A\} / \{(\kappa_1 + 1)(1 - \omega_d) k_A + k_{df}\} \\ &= [1 + \kappa_1 + k_{df} / \{(1 - \omega_d) k_A\}]^{-1} \\ f_{i^*} &= [1 + k_{df} / k_{th} + (k_{df} / k_A)(1 + k_{df} / k_{dd})]^{-1}, \end{aligned} \quad (69)$$

$$f_{i!} = \kappa_1 f_{i^*} \approx [1 + k_{th} / k_{df} + (k_{th} / k_A)(1 + k_{df} / k_{dd})]^{-1}, \quad (70)$$

$$\begin{aligned} f_{id} &= \{1 - (\kappa_1 + 1) f_{i^*}\} \omega_d \\ &\approx [1 + (k_{dd} / k_{df})(1 + k_A / k_{df} + k_A / k_{th})]^{-1}. \end{aligned} \quad (71)$$

The dimer formation and dissociation rates k_{df} and k_{dd} were given by Eqs (30) and (31), together with (21) through (27) and (32), while k_{th} was expressed by (55) and k_A by Eq (2).

Concentration fractions $f_{i!}$ and f_{id} given by (70) and (71) are key factors in isotope separation. The higher $f_{i!}$, the higher the enrichment factor β is. Note that at low temperatures with high levels of dimerization, one has $k_{dd} \ll k_{df}$ and $k_{dd} \rightarrow 0$. Then the third terms in the denominators of (69) and (70) approach infinity and both $f_{i!} \rightarrow 0$ and $f_{i^*} \rightarrow 0$, while $f_{id} \rightarrow 1$ according to (71). Finally note that unless $k_{dd} \rightarrow 0$, in the limit that $k_A \rightarrow \infty$, the population $f_{i!}$ becomes:

$$f_{i!} \rightarrow (1 + k_{th} / k_{df})^{-1} = \{1 + \mu_1 / (N_T \varphi_{df})\}^{-1}, \text{ for } k_A \gg k_{th}; k_{dd} > 0. \quad (72)$$

The ratio $k_{th} / k_{df} = \mu_1 / (N_T \varphi_{df})$ is clearly important, and the higher $N_T \varphi_{df}$ is, the higher $f_{i!}$ and β .

A second source term $+f_{i^*} (1 - x_i) (n_i / x_i) k_{VV}$ could have been added to the right-hand-side of (57) to represent VV re-transfers from other (non-*i*) excited ${}^i\text{QF}_6^*$ isotopomers which were produced by collisional VV transfers ${}^i\text{QF}_6^* +$

${}^j\text{QF}_6 \rightarrow {}^i\text{QF}_6 + {}^j\text{QF}_6^*$. Here $(1 - x_i) = x_j$ is the fraction of other isotopomers ${}^j\text{QF}_6$ ($j \neq i$), $n_i / x_i = n_Q$, k_{VV} is the VV transfer rate, and f_{i^*} is the steady-state fraction of isotopomers ${}^i\text{QF}_6^*$ that are excited due to VV transfers from ${}^i\text{QF}_6^*$. A second balance equation would have to be written for f_{i^*} , but if $y_Q = [\text{QF}_6] / [\text{G} + \text{QF}_6] < \sim 0.05$, the ‘‘VV recycle’’ term gives only a small correction and we shall (conservatively) neglect it.

We tacitly neglected laser excitation of epithermals or higher excitations of ${}^i\text{QF}_6^*$ molecules. If the kinetic energy ϵ_Q is high enough, it might be possible for an excited epithermal ${}^i\text{QF}_6^*$ to relax its ν_3 vibrational energy by direct VT conversion collisions, since φ_{VT} increases with T . However for ν_3 vibrations of QF_6 one finds $\epsilon_Q < 1000$ K, and the probability φ_{VT} is still negligible unless $M_{Q/G} < \sim 4$ amu (i.e., for $\text{G} = \text{H}_2$ or He). ‘‘In-flight’’ excited epithermals ${}^i\text{QF}_6^*$ must first slow down before they can dimerize and experience predissociation with VT conversion again. After thermalization, still-excited ${}^i\text{QF}_6^*$ become part of the thermal population group f_{i^*} , whose kinetics balance was already considered. Double and higher step excitations ${}^i\text{QF}_6^* \rightarrow {}^i\text{QF}_6^{**} \rightarrow {}^i\text{QF}_6^{***}$ can also occur, since absorption frequency differences for higher vibrational steps are usually small. However subsequent dimerization/VT conversion proceeds preponderantly in one-quantum steps, so we can lump f_{i^*} and $f_{i^{**}}$ populations with the f_{i^*} crowd.

5.2. Dimer laser excitation

If ${}^i\text{QF}_6:\text{G}$ dimers are laser-excited instead of ${}^i\text{QF}_6$ monomers, one can write:

$$f_{id} + f_{i!} + f_{im} = 1 \quad (73)$$

$$d(f_{id} n_i) / dt = (1 - f_{id} - f_{i!}) n_i k_{df} - f_{id} n_i (k_{dd} + k_A), \text{ s}^{-1} \text{ cm}^{-3}, \quad (74)$$

$$d(f_{i!} n_i) / dt = k_A f_{id} n_i - f_{i!} n_i \{(1 - e_1) k_{th} + e_1 k_{w1}\}, \text{ s}^{-1} \text{ cm}^{-3}. \quad (75)$$

Here f_{id} is the fraction of ${}^i\text{QF}_6$ that are dimerized as ${}^i\text{QF}_6:\text{G}$ and k_{dd} is the dimer dissociation rate given by (31). The laser rate k_A applies here to resonant absorptions by ${}^i\text{QF}_6:\text{G}$ dimers whose internal ν_3 vibrations are slightly shifted compared to the monomer ν_3 vibration of ${}^i\text{QF}_6$.

Under steady-state conditions, setting time derivatives equal to 0, one obtains:

$$f_{id} = k_{df} / \{(1 + \lambda_1) k_{df} + k_A + k_{dd}\} \approx k_{df} / \{(1 + \lambda_1) k_{df} + k_A\} \quad (76)$$

$$f_{i!} = \lambda_1 f_{id} \quad (77)$$

with:

$$\lambda_1 = k_A / \{(1 - e_1)k_{th} + e_1k_{w1}\} \approx k_A / k_{th}. \tag{78}$$

Usually $k_A \gg k_{dd}, k_{th} \gg e_1k_{w1}$, and $e_1 \ll 1$ if $p_G \sim 10^{-3}$ torr, in which case the approximations in (76) and (78) apply. Combining (76) and (77) yields:

$$\begin{aligned} f_{i;d} \equiv (f_{i'})_d &= k_A k_{df} / [k_A \{k_{df} + (1 - e_1)k_{th} + e_1k_{w1}\} \\ &\quad + (k_{df} + k_{dd})\{(1 - e_1)k_{th} + e_1k_{w1}\}] \\ &\approx k_A k_{df} / \{k_A(k_{df} + k_{th}) + k_{th}(k_{df} + k_{dd})\} \\ &= [1 + k_{th}/k_{df} + (k_{th}/k_A)(1 + k_{dd}/k_{df})]^{-1}, \end{aligned} \tag{79}$$

and:

$$f_{i;d} \equiv (f_{id})_d = f_{i'} / \lambda_1 \approx [1 + k_A/k_{th} + k_A/k_{df} + k_{dd}/k_{df}]^{-1}. \tag{80}$$

Here we added subscripts d to $f_{i'}$ and f_{id} to distinguish dimer laser-excitation fractions $f_{i;d}$ and $f_{i;d}$ from expressions for monomer laser-excitation fractions $f_{i'}$ and f_{id} given in Section 5.1.

Comparing (79) with (70), we see that the expressions for $f_{i;d}$ and $f_{i'}$ are almost the same except for the last term in the bracket. For dimer-excitation the last term $k_{dd}/k_{df} \rightarrow 0$ if $k_{dd} \rightarrow 0$, and:

$$f_{i;d} \rightarrow [1 + k_{th}/k_{df} + k_{th}/k_A]^{-1}, \text{ for } k_{dd} \rightarrow 0. \tag{81}$$

On the other hand, for monomer pumping we found $f_{i'} \rightarrow 0$ when $k_{dd} \rightarrow 0$ since the last term $k_{df}/k_{dd} \rightarrow \infty$. Thus at very low temperatures where $k_{dd} \rightarrow 0$, only laser excitation of ${}^i\text{QF}_6$ dimers can promote isotope separation. However because monomers have higher and sharper peak absorption cross-sections (σ_A) than dimers, it is more advantageous to pump monomers instead of dimers, as long as k_{dd} is not entirely 0. That is, with the same laser intensity or flux φ_L , one usually finds $(k_A)_{\text{monomer}} \sim 10(k_A)_{\text{dimer}}$. Temperatures and pressures for optimum enrichments using either monomer or dimer laser pumping will be analyzed in the next section.

6. LASER-INDUCED ISOTOPE SEPARATIONS IN SKIMMER-SCOOPED JETS

6.1. Enrichment factor β_m for monomer laser excitations

Assuming continuous laser irradiation of the jet and steady jet flow, the mole fractions of thermals (${}^i\text{QF}_6 + {}^i\text{QF}_6^*$), epithermals (${}^i\text{QF}_6'$), and thermal dimers ${}^i\text{QF}_6:\text{G}$ throughout the jet will be $f_{it}x_i y_Q = (1 - f_{i'} - f_{id})x_i y_Q, f_{i'}x_i y_Q$, and $f_{id}x_i y_Q$, where y_Q is the mole fraction of QF_6 in the gas mix and $x_i = [{}^i\text{QF}_6] / [\sum_j ({}^j\text{QF}_6)]$ is the isotopic abundance of ${}^i\text{QF}_6$. Here

the fraction of excited and non-excited thermal monomers is $f_{it} = f_{i'} + f_{im} = 1 - f_{i'} - f_{id}$. Fractions $f_{it}, f_{i'}, f_{id}, f_{jt}$, and f_{jd} are constant but the number of ${}^i\text{QF}_6$ and ${}^j\text{QF}_6$ in the jet drops as the jet travels through the chamber to the skimmer due to escape fractions Θ, Θ_1 , and Θ_d .

Using a prime to label the isotopic abundance of ${}^i\text{QF}_6$ in core-escaped gas and no prime for incoming un-irradiated feed gas, the isotopic composition x_i' of QF_6 in the escaped gas is:

$$\begin{aligned} x_i' &= [\text{All escaped } {}^i\text{QF}_6] \div [\text{All escaped } \text{QF}_6] \\ &= [x_i \{(1 - f_{i'} - f_{id})\Theta + f_{i'}\Theta_1 + f_{id}\Theta_d\}] \\ &\quad \div [(1 - x_i)\{(1 - f_{jd})\Theta + f_{jd}\Theta_d\}] \\ &\quad + x_i \{(1 - f_{i'} - f_{id})\Theta + f_{i'}\Theta_1 + f_{id}\Theta_d\}, \end{aligned} \tag{82}$$

or:

$$\begin{aligned} \beta_m = x_i' / x_i &= \{1 + f_{i'}(\phi_1 - 1) - f_{id}(1 - \phi_d)\} / [1 - \omega_d(1 - \phi_d) \\ &\quad + x_i \{\omega_d(1 - \phi_d) + f_{i'}(\phi_1 - 1) - f_{id}(1 - \phi_d)\}] \\ &= [1 - \omega_d(1 - \phi_d)\{1 - (\kappa_1 + 1)f_{i'}\} + \kappa_1 f_{i'}(\phi_1 - 1)] / \\ &\quad \times [1 - \omega_d(1 - \phi_d) + x_i f_{i'}\{(\phi_1 - 1)\kappa_1 \\ &\quad + \omega_d(1 - \phi_d)(\kappa_1 + 1)\}]. \end{aligned} \tag{83}$$

Here $\beta_m = x_i' / x_i$ is the enrichment factor for ${}^i\text{QF}_6$ in the jet-escaped rim gases, and ϕ_1, ϕ_d equal:

$$\begin{aligned} \phi_1 = \Theta_1 / \Theta &= \{1 - \exp(-k_{w1} t_{tr})\} / \{1 - \exp(-k_w t_{tr})\} \\ &= \{1 - \exp(-\mu_1 k_w t_{tr})\} / \{1 - \exp(-k_w t_{tr})\}, \end{aligned} \tag{84}$$

$$\begin{aligned} \phi_d = \Theta_d / \Theta &= \{1 - \exp(-k_{wd} t_{tr})\} / \{1 - \exp(-k_w t_{tr})\} \\ &= \{1 - \exp(-\psi_d k_w t_{tr})\} / \{1 - \exp(-k_w t_{tr})\}. \end{aligned} \tag{85}$$

Parameters $\mu_1, \psi_d, \kappa_1, \omega_d$, and k_w were given by (40), (47), (66), (68), and (34), while mole fractions $f_{i'}, f_{i'}$, and f_{id} were given by (69), (70), and (71). Mole fractions f_{jm} and f_{jd} of other isotopic monomers ${}^j\text{QF}_6$ and dimers ${}^j\text{QF}_6:\text{G}$ are:

$$\begin{aligned} f_{jm} = 1 - f_{jd} &= 1 - \omega_d = k_{dd} / (k_{df} + k_{dd}) = (1 + k_{df}/k_{dd})^{-1} \\ &= \{1 + \varphi_{df} / (a_d \varphi_{dd})\}^{-1}, \end{aligned} \tag{86}$$

$$\begin{aligned} f_{jd} = \omega_d &= k_{df} / (k_{df} + k_{dd}) = (1 + k_{dd}/k_{df})^{-1} \\ &= (1 + a_d \varphi_{dd} / \varphi_{df})^{-1}, \end{aligned} \tag{87}$$

with escape fractions Θ and Θ_d . Also of course $x_j = 1 - x_i$. Note that f_{jd} given by (87) agrees with f_{id} expressed by (71) for $k_A = 0$. Also note if $x_i \ll 1$, the enrichment factor becomes:

$$\beta_m \approx 1 + f_{i^*} \{ \kappa_1 (\phi_1 - 1 + c_d) + c_d \} / (1 - c_d), \quad (x_i \ll 1) \quad (88)$$

with:

$$c_d = \omega_d (1 - \phi_d). \quad (89)$$

The enrichment relation (83) or (88) has three important components, f_{i^*} , ϕ_1 , and c_d . The laser-pumped excited fraction f_{i^*} increases with laser radiation intensity and the higher f_{i^*} is, the higher β_m . However f_{i^*} also depends on the availability of monomers and, as mentioned, if $k_{dd} \rightarrow 0$ or $\omega_d \rightarrow 1$, one finds $f_{i^*} \rightarrow 0$. This happens at low temperatures when all monomers become dimerized during the jet flight and there are no monomers left for laser excitation. Since the factor f_{i^*} can never exceed 1, only the epithermal factor ϕ_1 and dimer factor c_d can make β_m larger than 2. The larger ϕ_1 and c_d are, the higher β_m is.

Figures 4 and 5 show plots of β_m at different pressures and temperatures for several SF₆/G and UF₆/G gas mixtures, assuming a fixed $k_A = 10^5 \text{ s}^{-1}$ and jet core with radius $R = 1 \text{ cm}$ and length $L = 20 \text{ cm}$. The curves show maximum β_m 's around $T = 25 \text{ K}$ for SF₆/G and $T = 35 \text{ K}$ for UF₆/G at pressures between $p_G = 0.005$ and 0.05 torr . High values of β are driven by high values for c_d and ϕ_1 . The latter has high values when $\epsilon_Q/\epsilon_T = \eta_{Q/G} \epsilon_a / (kT)$ is high. Since ϵ_a is fixed for a given QF₆, one expects low values of T and a high

value for $\eta_{Q/G} = M_G / (M_G + M_Q)$, (i.e., high M_G), to yield a high ϕ_1 and β . Indeed Figures 4 and 5 show heavy SiBr₄ ($M_G = 348$) as carrier to give the highest enrichment, but its poor aerodynamics gives problems (see Sections 7 and 8). Low temperatures for good enrichments can only be attained temporarily in supersonic jets. Feasibility of attaining such low temperatures will be investigated in Section 7.

Inspection of (83) and (88) shows that the observed peaks of β_m around $T = T_{\max} \sim 25 \text{ K}$ for SF₆/G and $T = T_{\max} \sim 35 \text{ K}$ for UF₆/G, occur just before $\omega_d \rightarrow 1$ or $\omega_d \approx 0.995$, where:

$$\phi_{dd}(T) \sim 0.005 \phi_{df}(T), \quad (\text{maximum } \beta_m). \quad (90)$$

For T much less than T_{\max} , almost total dimerization occurs as $\omega_d \rightarrow 1$ or $\phi_{dd} \ll \phi_{df}$. Under these strong dimerization conditions, there are no monomers left for laser excitation during the supersonic jet flight in the chamber, and thus $\beta \rightarrow 1$. One finds that epithermals contribute very little to β_{\max} , and the major isotopic effect is due to dimers.

6.2. Enrichment factor β_d with dimer laser excitation

Isotope enrichment factors under direct selective laser excitation of dimers ⁱQF₆:G can be deduced in the same manner

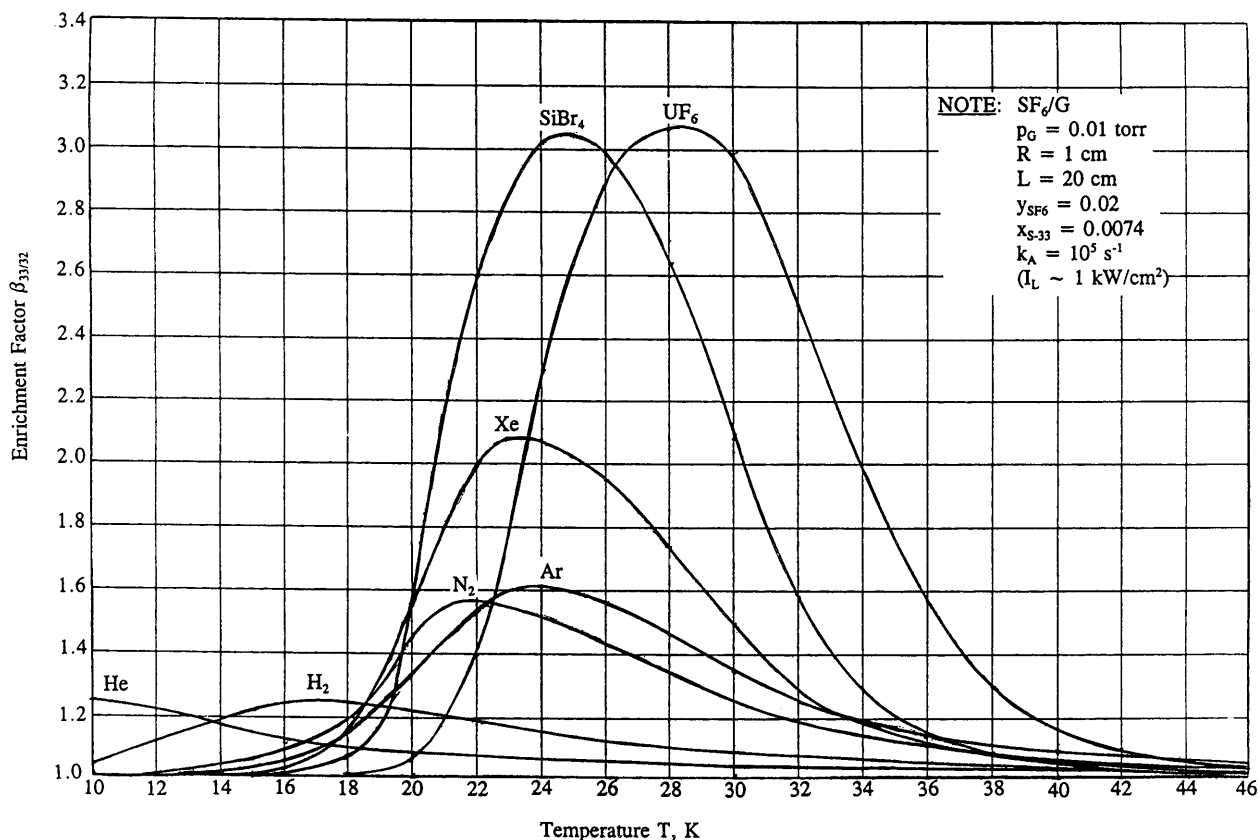


Fig. 4A. Enrichment factors $\beta_m(T)$ for SF₆(ν_3) monomer excitation at fixed p_G .

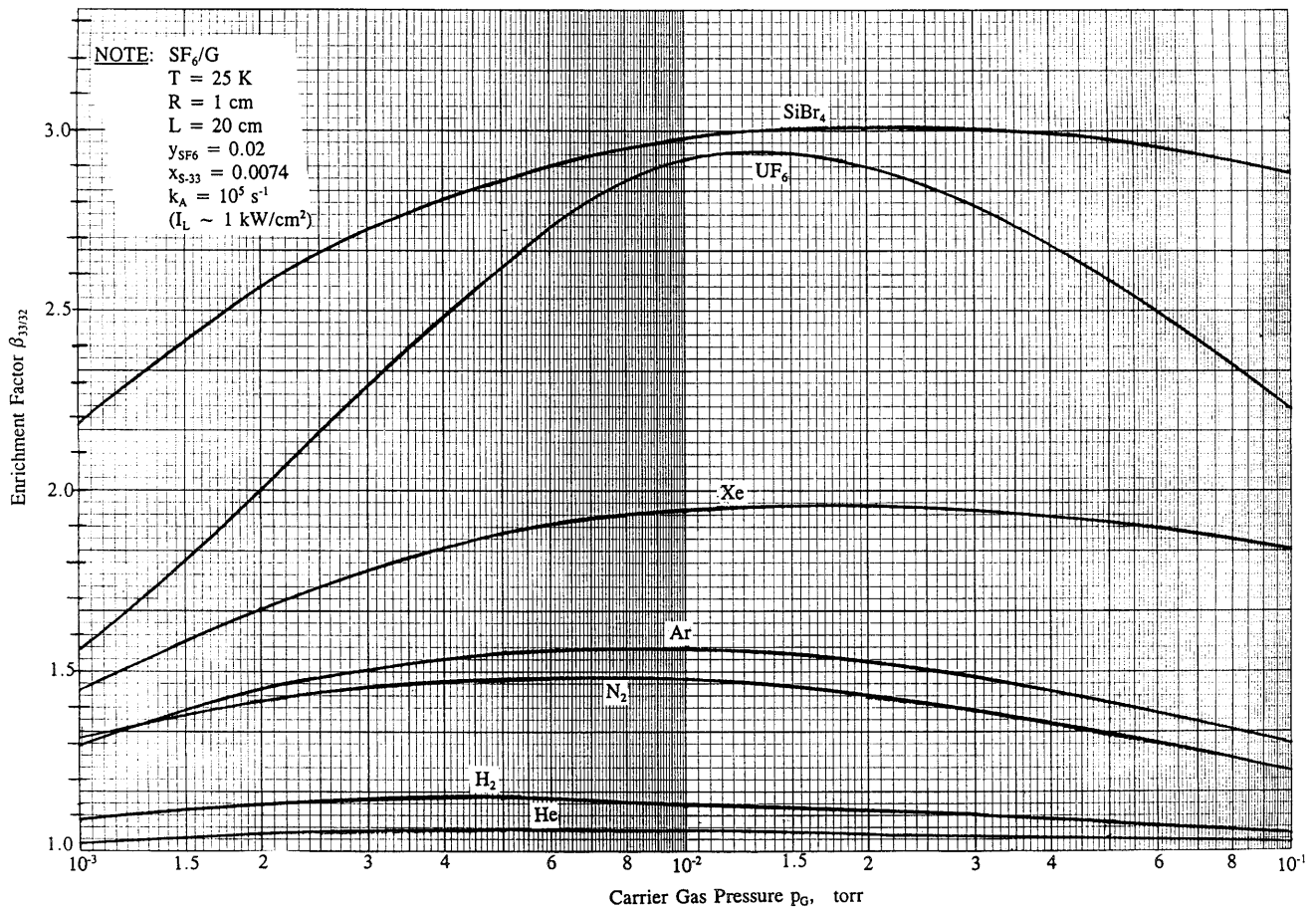


Fig. 4B. Enrichment factors $\beta_m(p_G)$ for $SF_6(\nu_3)$ monomer excitation at fixed T .

using the fractions f_{idd} and $f_{i|d}$ obtained in Section 5.2. One has:

$$\beta_d = [(1 - f_{i|d} - f_{idd})\Theta + f_{i|d}\Theta_1 + f_{idd}\Theta_d]/$$

$$\times [(1 - x_i)\{\omega_d\Theta_d + (1 - \omega_d)\Theta\}$$

$$+ x_i\{(1 - f_{i|d} - f_{idd})\Theta + f_{i|d}\Theta_1 + f_{idd}\Theta_d\}]$$

$$= [1 + \{(\phi_1 - 1)\lambda_1 - 1 + \phi_d\}f_{idd}]/$$

$$\times [1 - c_d(1 - x_i) + x_i f_{idd}\{(\phi_1 - 1)\lambda_1 - 1 + \phi_d\}], \quad (91)$$

where $\lambda_1 (\approx k_A/k_{th})$, ϕ_1 , ϕ_d , and $c_d = \omega_d(1 - \phi_d)$ were given, respectively, by (78), (84), (85), and (89) with $\omega_d = k_{df}/(k_{df} + k_{dd})$ defined by (68), and where $f_{idd} = [1 + k_A/k_{th} + k_A/k_{df} + k_{dd}/k_{df}]^{-1}$ was given by (80). For $x_i \ll 1$, the expression for β_d reduces to:

$$\beta_d = [1 + \{(\phi_1 - 1)\lambda_1 - 1 + \phi_d\}f_{idd}]/(1 - c_d), \quad (x_i \ll 1). \quad (92)$$

For low temperatures where $k_{dd} \ll k_{df}$ and $\omega_d \rightarrow 1$, one has that $c_d \rightarrow (1 - \phi_d)$ and (92) becomes:

$$\beta_d = [1 + \{(\phi_1 - 1)\lambda_1 - 1 + \phi_d\}f_{idd}]/\phi_d, \quad (x_i \ll 1; k_{dd} \ll k_{df}) \quad (93)$$

with:

$$f_{idd} = [1 + k_A/k_{th} + k_A/k_{df}]^{-1} \quad (k_{dd} \ll k_{df}). \quad (94)$$

Figures 6 and 7 show enrichment factors $\beta_d(T)$ for $^{33}SF_6/G$ and $^{235}UF_6/G$ for carriers Ar and Xe at various temperatures and pressures, assuming $R = 0.4$ cm and a laser excitation rate of $k_A = 10^4$ s $^{-1}$ (simulating $(\sigma_A)_{dimer} \sim 0.1$ ($\sigma_A)_{monomer}$). The plots show peaks of β_d in the same general region (20–40 K) where β_m peaks, but in addition there are some high β_d values at very low pressures ($p_G \sim 0.001$ torr) and temperatures ($T < \sim 0.5$ K), where complete dimerization has set in. This region is unattractive however since such low jet expansion temperatures and pressures are difficult (costly) to achieve, and product cuts Θ_o are very low there (see below).

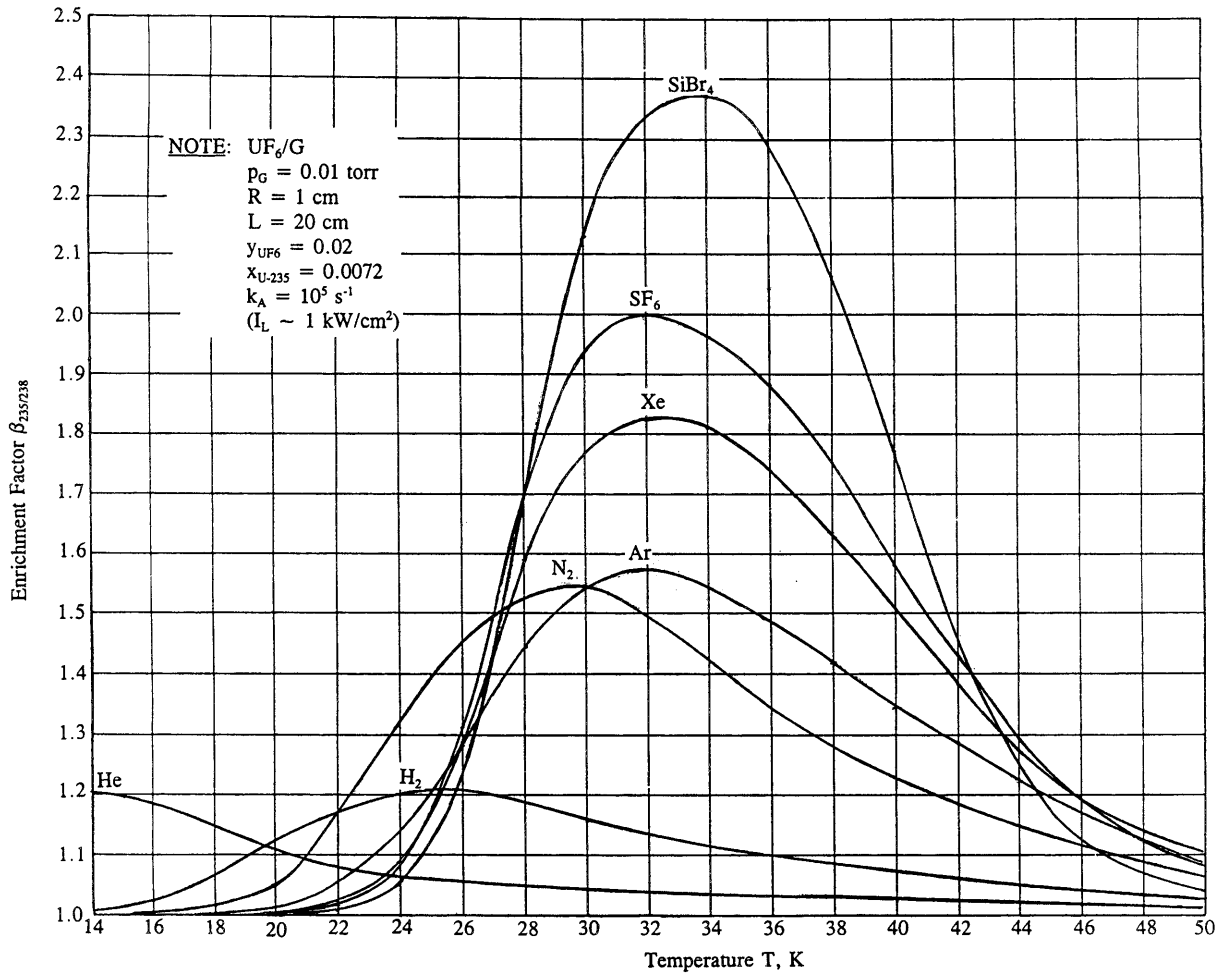


Fig. 5A. Enrichment factors $\beta_m(T)$ for $UF_6(\nu_3)$ monomer excitation at fixed p_G .

6.3. Overall product cuts Θ_o for monomer and dimer excitations and depletion factor γ

The enrichment factor β alone is insufficient to characterize the performance of an isotope separation process and a minimum of two performance parameters are needed. Besides β , the product “cut” Θ or tails isotope depletion factor γ must be specified to define a separation process (Benedict *et al.*, 1981). Usually the product output cut Θ_o is specified which is defined by:

$$\Theta_o = \frac{[\text{Quantity of } QF_6 \text{ in Enriched Product Stream}]}{[\text{Quantity of } QF_6 \text{ in Feed Stream}]} = \text{Total Fractional Loss of } QF_6 \text{ from the Jet Core.} \quad (95)$$

From a mass balance, one can show that the isotope depletion factor γ in the “Tails” stream (this γ not to be confused with $\gamma = c_p/c_v$) is related to β and Θ_o by (Benedict, 1981):

$$\begin{aligned} \gamma &= \frac{[{}^iQF_6]/[QF_6]_{\text{Tails}}}{[{}^iQF_6]/[QF_6]_{\text{Feed}}} \\ &= [1 - \Theta_o\{1 + (1 - x'_i)(\beta - 1)\}] \\ &\quad \div [1 - (\Theta_o/\beta)\{1 + (1 - x'_i)(\beta - 1)\}] \\ &= x''_i/x_i \approx (1 - \beta\Theta_o)/(1 - \Theta_o), \text{ if } x'_i \ll 1. \end{aligned} \quad (96)$$

Here a single prime refers to product, a double prime to tails, and no prime to the feed stream.

In the case of monomer excitations, the product cut Θ_{om} according to (95) equals:

$$\Theta_{om} = x_i(f_{it}\Theta + f_{i1}\Theta_1 + f_{id}\Theta_d) + x_j(f_{jm}\Theta + f_{jd}\Theta_d), \quad (97)$$

which reduces to:

$$\Theta_{om} = \Theta[1 - c_d + x_i f_{i*}\{(\phi_1 - 1)\kappa_1 + c_d(\kappa_1 + 1)\}], \quad (98)$$

where $\Theta = 1 - \exp(-k_w t_{tr})$, $\Theta_1 = 1 - \exp(-\mu_1 k_w t_{tr})$, $\Theta_d = 1 - \exp(-\psi_d k_w t_{tr})$, $\phi_1 = \Theta_1/\Theta$, $\phi_d = \Theta_d/\Theta$ (see Eqs (37), (45), (48), (84), (85)). The parameter $c_d = \omega_d(1 - \phi_d)$ was

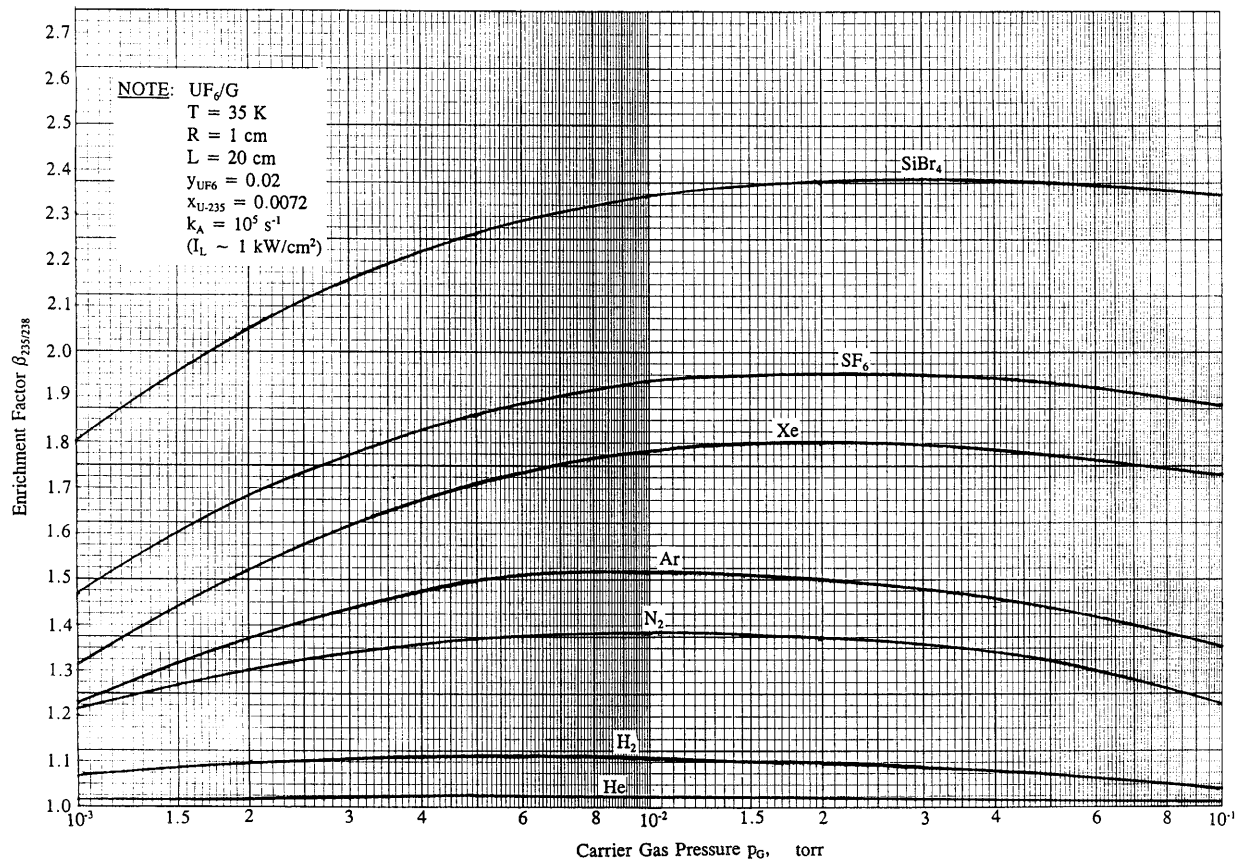


Fig. 5B. Enrichment factors $\beta_m(p_G)$ for $UF_6(\nu_3)$ monomer excitation at fixed T .

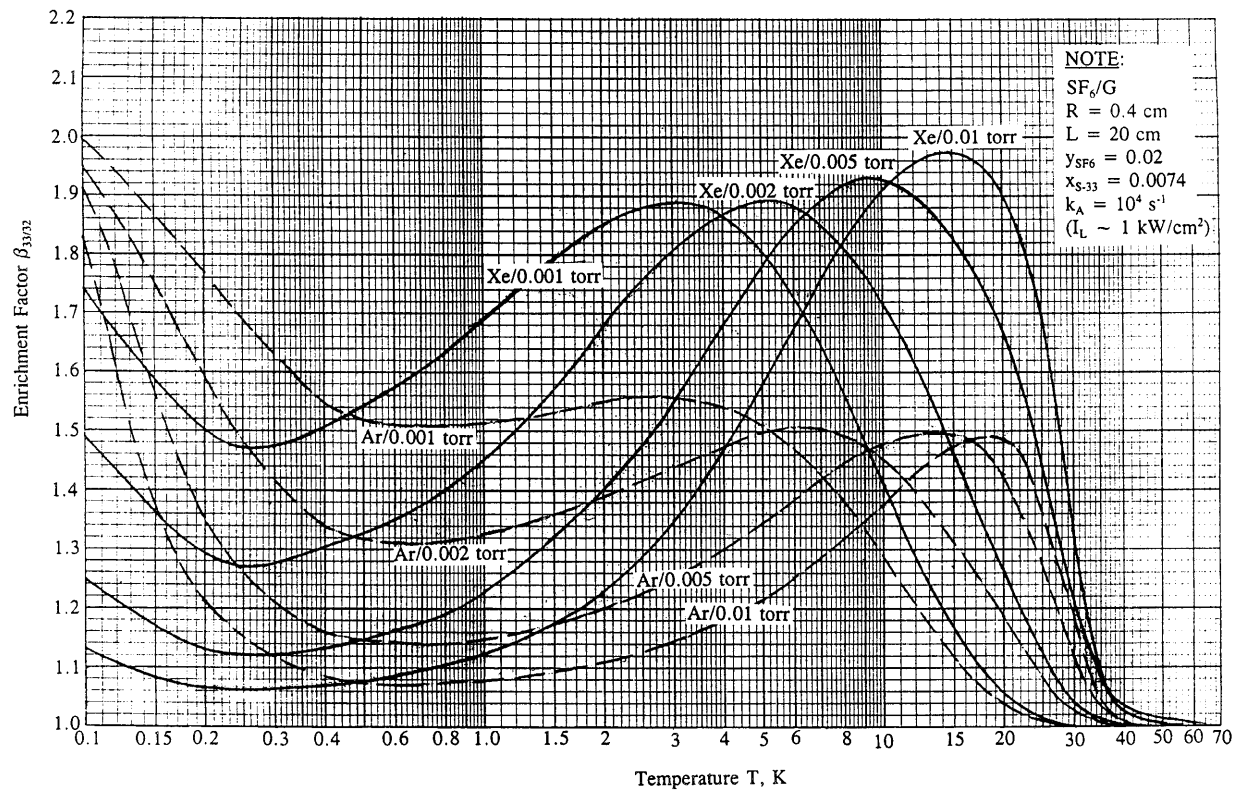


Fig. 6. Enrichment factors $\beta_d(p_G, T)$ for $SF_6:G$ dimer laser excitations.

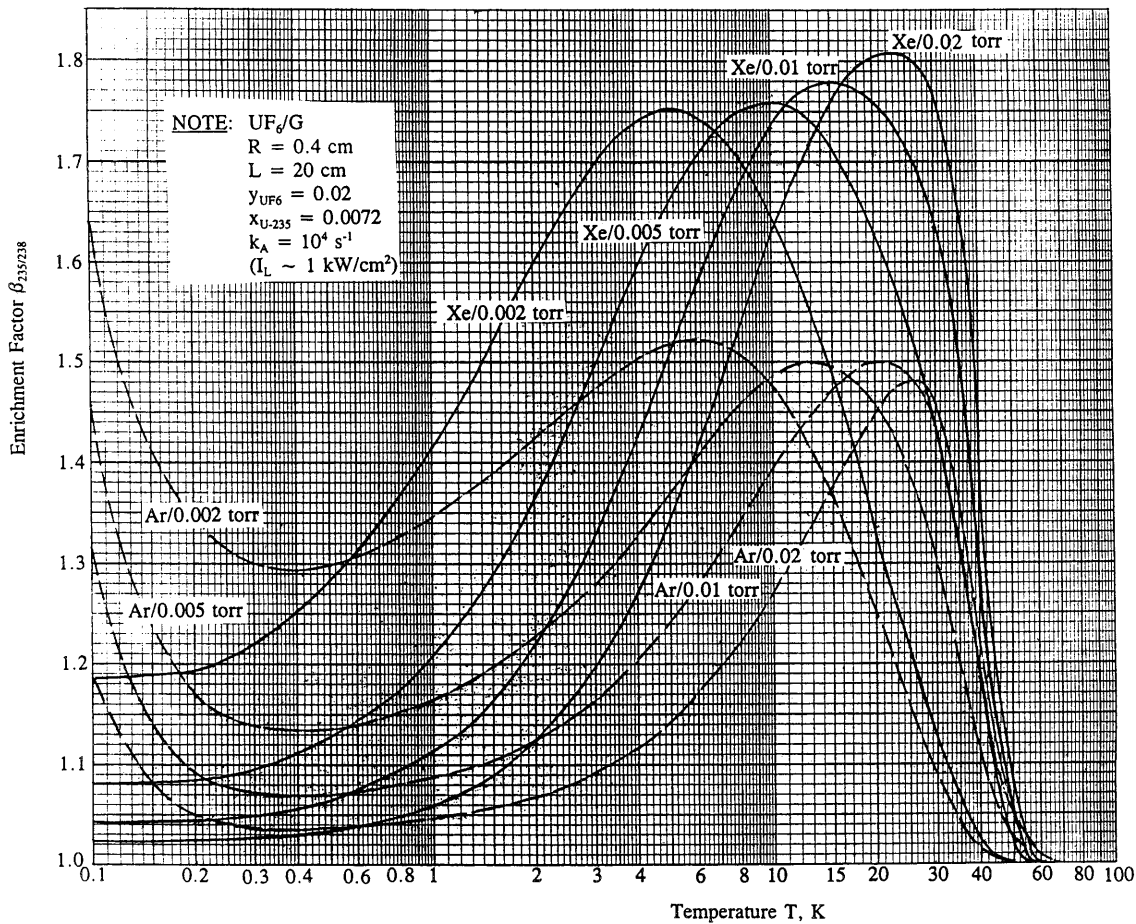


Fig. 7. Enrichment factors $\beta_d(p_G, T)$ for $UF_6:G$ dimer laser excitations.

previously defined by (89), $\omega_d = k_{df}/(k_{df} + k_{dd})$ by (68), while fractions $f_{it} = f_{im} + f_{i^*} = 1 - f_{i'} - f_{id}$, $f_{i'} = \kappa_1 f_{i^*}$, and $f_{id} = \omega_d \{1 - (\kappa_1 + 1) f_{i^*}\}$, with f_{i^*} given by (69) and κ_1 by (66). We also used the relations $x_j = 1 - x_i$, $f_{jd} = \omega_d$, and $f_{jm} = 1 - f_{jd} = 1 - \omega_d$.

For the dimer excitation case, one deduces similarly:

$$\Theta_{od} = \Theta [1 - c_d + x_i \{ (\phi_1 - 1) \lambda_1 f_{idd} - (1 - \phi_d) f_{idd} + c_d \}], \quad (99)$$

where $\lambda_1 \approx k_A/k_{th}$ was given by (80) and f_{idd} by (82).

If $x_i \ll 1$, both Θ_{om} and Θ_{od} reduce to:

$$\Theta_{om} \approx \Theta_{od} \approx \Theta_o = (1 - c_d) \Theta, \quad (\text{for } x_i \ll 1) \quad (100)$$

with Θ given by (37) and ω_d by (89). Figures 8 and 9 give calculated curves of Θ_o for SF_6/G and UF_6/G in the pressure and temperature ranges where β_m and β_d are high. For $\Theta_o > \sim 0.3$, the cylindrical jet approximation may become less realistic, and the equations for calculating β_m , β_d , and Θ_o are less reliable. Note that at temperatures below $T = 1 \text{ K}$,

where β_d has some secondary peaks, the product cuts Θ_o are very small ($\Theta_o < \sim 10^{-3}$), and economically unattractive.

For a usable laser isotope separation process, one would like $\Theta_o > \sim 0.08$ and $\beta > \sim 1.8$ or $\gamma < \sim 0.93$ according to (96). From Figs. 4 through 9, it is clear that cuts Θ_o are higher the higher T and p are, contrary to the enrichment factor β which is higher the lower T and p are. Thus compromise temperatures and pressures must be chosen to optimize separations. For example for SF_6/Xe , one might select $T = 25 \text{ K}$ and $p_{Xe} = 0.007 \text{ torr}$, which gives $\beta = 2.00$ and $\Theta_o = 0.10$. For UF_6/SF_6 , a possible selection might be $T = 35 \text{ K}$, $p_{SF_6} = 0.02 \text{ torr}$, yielding $\beta = 1.95$, $\Theta_o = 0.23$. These are reasonable process parameters, and allow $^{33}SF_6$ to be enriched from 0.75% to 96% in seven stages for example, or $^{235}UF_6$ from 0.73% to 2.8% in two, or from 0.73% to 5.4% in three stages. This is much better than in Diffusion ($\beta \sim 1.002$) or Ultracentrifuge ($\beta \sim 1.1$) separation plants that enrich $^{235}UF_6$ employing hundreds of stages.

For the MLIS/CRISLA scheme, staging is simple since Feed, Product, and Tails streams are all gaseous and chemically the same except for isotope concentrations. In MLIS

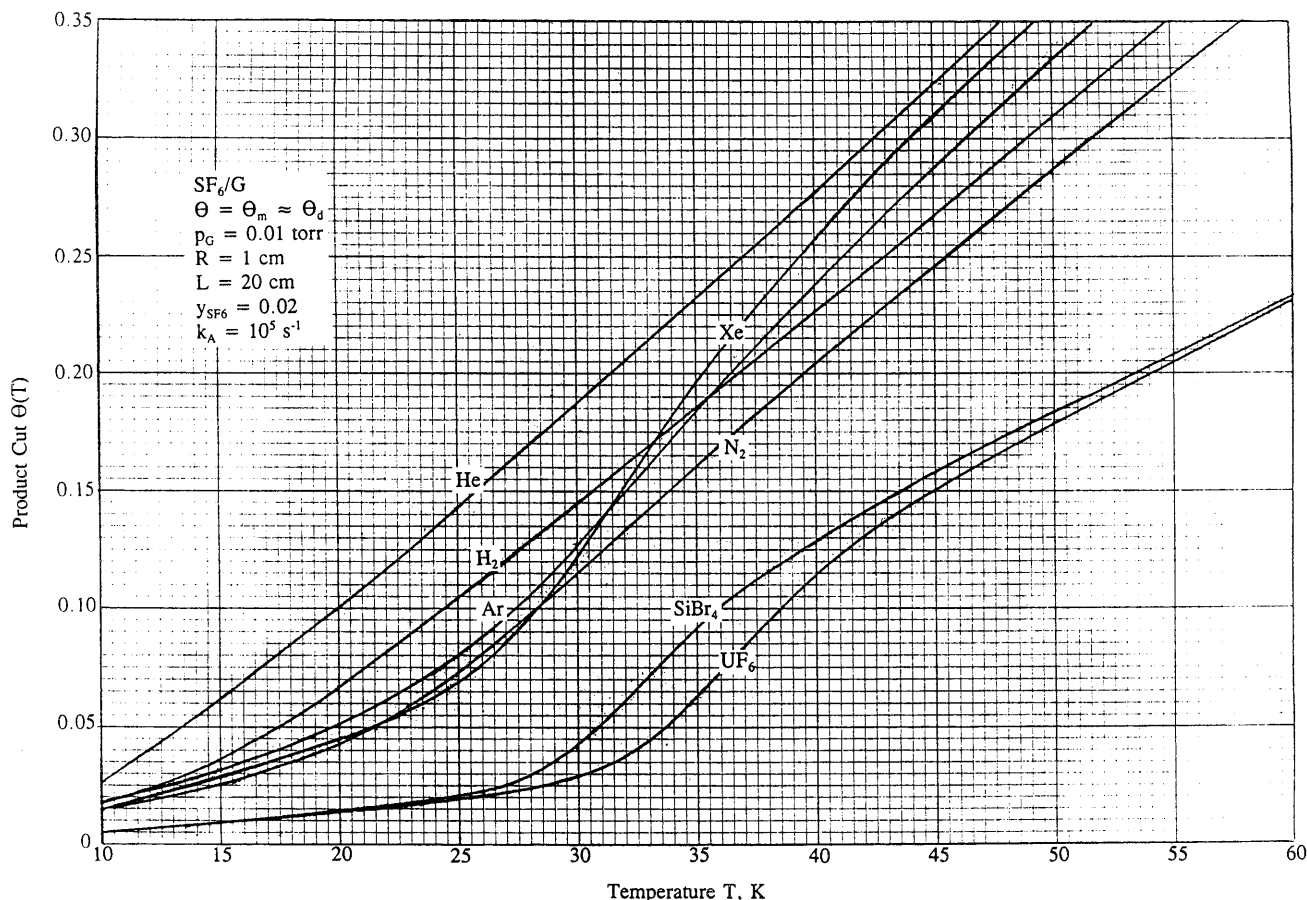


Fig. 8A. Isotope product cuts $\Theta(T)$ for $^{33}\text{SF}_6$ at fixed p_G .

schemes other than CRISLA, the product is chemically changed and must be reformed between stages.

7. SUPERSONIC FLOW AND SUPERSATURATION CONSIDERATIONS

7.1. Free jet flow characteristics

To ascertain that the free-jet low temperatures and pressures desirable for useful isotope separations are attainable without excessive cluster growth, we briefly examine some supersonic expansion relations obtained from the adiabatic expansion relations (Liepmann & Puckett, 1953):

$$T/T_o = (p/p_o)^{(\gamma-1)/\gamma} = (n/n_o)^{(\gamma-1)} \tag{101}$$

$$(A/A_t)^2 = \frac{1}{2}(\gamma - 1)\{2/(\gamma + 1)\}^{(\gamma+1)/(\gamma-1)}(p_o/p)^{2/\gamma} \times \{1 - (p/p_o)^{(\gamma-1)/\gamma}\}^{-1} \tag{102}$$

$$(U/U_{so})^2 = \{2/(\gamma - 1)\}(1 - T/T_o). \tag{103}$$

Here subscripts o and t on T, p, A refer to upstream reservoir (stagnation) and throat conditions of the gas mixture which

is expanded from a large reservoir through a small constricting circular opening or a slit (the “throat”) with cross-sectional area A_t . No subscripts indicate downstream conditions in the supersonic jet stream. A is the cross-sectional area through which the jet core flows and U is the supersonic bulk-flow velocity of the jet at a downstream station. U_{so} is the sound velocity of the gas in the reservoir, given by (Liepmann, 1953):

$$U_{so} = 9,116.5 \{ \gamma T_o(\text{K})/M(\text{amu}) \}^{1/2}, \text{ cm/s}, \tag{104}$$

with M being the atomic mass of the gas atoms or molecules in amu. Gas coefficients $\gamma = c_p/c_v$ equal $\gamma = 1.67$ for monatomics He, Ar, Xe, $\gamma = 1.4$ for diatomic gases (H_2 and N_2), $\gamma \approx 1.3$ for SF_6 , CH_4 , and Br_2 , and $\gamma \approx 1.07$ for UF_6 and SiBr_4 .

Low-pressure background gases in the jet chamber create a diffuse boundary layer around an expanding supersonic free-jet core, as the latter experiences oscillating expansions and contractions that form a series of Mach cells with normal and oblique shocks. Figures 10 and 11 show free-jet structures measured by (Eerkens, 1957, 1958) and (Chow, 1959) for reservoir pressures of $p_o = 0.8$ and 3.9 torr, and throat diameters of $D_t = 2.22$ and 1.27 cm, with jets exhaust-

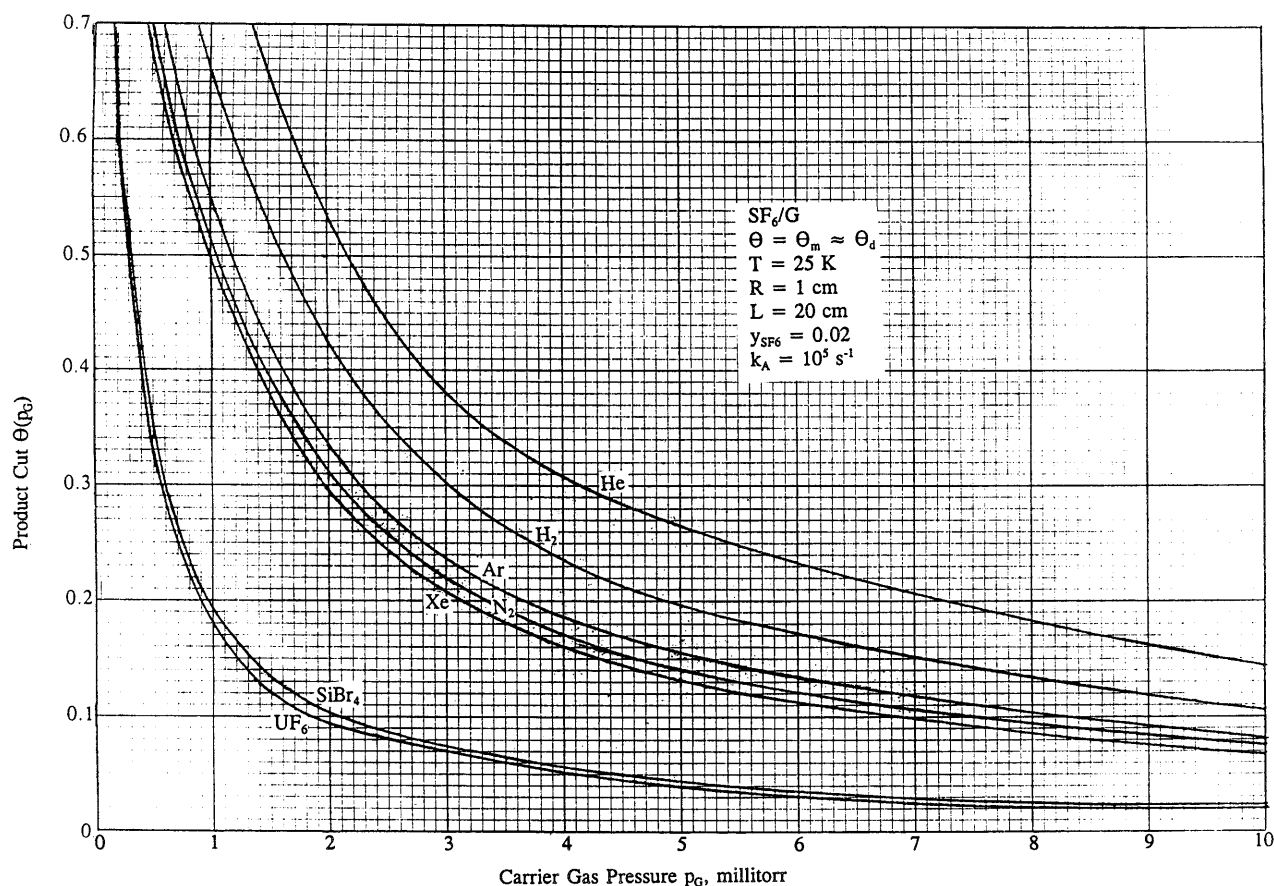


Fig. 8B. Isotope product cuts $\Theta(p_G)$ for $^{33}SF_6$ at fixed T .

ing into vacuum chambers pumped down to less than 0.01 torr. The latter conditions are close to the expansions needed for successful CRISLA operations. The jet contours of Figures 10 and 11 also show that it is reasonable to approximate the jet core by a gas-filled cylinder with a “vacuum wall” as assumed in Section 4.2 to simplify mathematics. As long as radial diffusion losses from the jet are not excessive ($\Theta_0 \leq \sim 0.3$), jet expansion parameters using (101)–(104) provide useful first-order estimates. Note that because the flow is supersonic, the downstream skimmer (see Fig. 1), can not perturb the upstream flow pattern.

Theoretical calculations of two-dimensional jets, though available (Adamson & Nichols, 1959), are complex and involve graphical constructions. While the one-dimensional flow relations (101)–(104) can not predict the observed two-dimensional “Mach diamonds or cells” of supersonic free jets, they do provide average order-of-magnitude downstream values of the supersonic flow expansion cross-sections (A/A_1) and accompanying pressures and temperatures. To attain gas expansions to $T \sim 25 \text{ K}$ and $p \sim 0.01$ torr with a noble gas carrier for example, one calculates reservoir pressures of 5 torr and throat diameters of 0.532 cm, which are quite manageable. Table 4 lists calculated values of the required reservoir tank pressures p_0 and required circular throat radii R_1 or rectangular slit widths W_1 , for various

carrier gases containing a few percent QF_6 , which are expanded in one step to pressure $p = 0.01$ torr and various temperatures in a vacuum chamber. The reservoir temperature is assumed to be $T_0 = 300 \text{ K}$ in these one-step-expansion calculations, while a final jet radius of $R_j = 1 \text{ cm}$ is assumed in all cases. Calculations with $SiBr_4$ as carrier gas G shows it to be impractical due to a very low γ . Low-energy vibrations ($h\nu_a \sim kT$) in this molecule retain too much energy at low temperatures.

To improve laser beam overlap and flow control, it can be advantageous to pass the gas first through a contoured supersonic nozzle, before allowing it to expand as a free jet into the jet chamber, as illustrated in Figure 1. The gas can be pre-expanded smoothly in a nozzle (with less flaring) for example from ~ 5 torr at $T = 300 \text{ K}$ in the feed chamber to about 0.1 torr and $T \sim 63 \text{ K}$ at the nozzle exit, using an axi-symmetric Mach-3.4 nozzle with exit diameter of 0.6 cm (including boundary layer) and throat diameter of 0.26 cm. The gas mix subsequently enters the jet chamber where it expands further to $p \approx 0.005$ torr and $T \sim 25 \text{ K}$ with some flaring, forming a quasi-cylindrical jet. Actually any available Mach-3 or Mach-4 supersonic nozzle with throat radius 0.2–0.5 cm and exit radius 5–7 cm can be adapted for this function.

For increased flow rates slit nozzles with two-dimensional (instead of axisymmetric) jets can be used. In this case, the

Table 4. Calculated one-step supersonic jet expansion parameters for QF_6/G with $G = \text{He, Ar, Xe}$ ($\gamma = 1.67$); $G = \text{H}_2, \text{N}_2$ ($\gamma = 1.4$); $G = \text{SF}_6$ ($\gamma = 1.33$); $G = \text{SiBr}_4$ ($\gamma = 1.07$)^a

Parameter	Monatomic Gases with $\gamma = 1.667$ G = He, Ar, Xe			Diatomic gases with $\gamma = 1.4$ G = H ₂ , N ₂			Polyatomic Gas G = SF ₆ with $\gamma = 1.33$			Polyatomic Gas G = SiBr ₄ with $\gamma = 1.07$		
	Expansion Temperature T			Expansion Temperature T			Expansion Temperature T			Expansion Temperature T		
	25 K	35 K	55 K	25 K	35 K	55 K	25 K	35 K	55 K	25 K	35 K	55 K
Reservoir p_0 , torr	5.00	2.15	0.695	59.9	18.44	3.79	223.4	57.57	9.314	3×10^{14}	1.8×10^{12}	1.8×10^9
R_{throat} , cm	0.266	0.340	0.467	0.086	0.117	0.224	0.0466	0.077	0.149	6×10^{-7}	6.3×10^{-7}	1.6×10^{-5}
W_{throat} , cm	0.0708	0.115	0.218	0.0075	0.0136	0.053	0.0022	0.006	0.022	3×10^{-15}	4×10^{-13}	2.4×10^{-10}
U_{st} , km/s ^b	0.883 (He)	0.883 (He)	0.883 (He)	1.206 (H ₂)	1.206 (H ₂)	1.206 (H ₂)	0.140	0.140	0.140	0.0861	0.0861	0.0861
	0.279 (Ar)	0.279 (Ar)	0.279 (Ar)	0.322 (N ₂)	0.322 (N ₂)	0.322 (N ₂)						
	0.154 (Xe)	0.154 (Xe)	0.154 (Xe)									
U , km/s	1.690 (He)	1.659 (He)	1.596 (He)	2.828 (H ₂)	2.777 (H ₂)	2.670 (H ₂)	0.3552	0.349	0.335	0.4481	0.4399	0.4230
	0.535 (Ar)	0.524 (Ar)	0.504 (Ar)	0.756 (N ₂)	0.742 (N ₂)	0.714 (N ₂)						
	0.295 (Xe)	0.290 (Xe)	0.278 (Xe)									
t_{tr} , ms ^c	0.156 (He)	0.157 (He)	0.161 (He)	0.099 (H ₂)	0.100 (H ₂)	0.103 (H ₂)	0.8084	0.819	0.842	0.7488	0.7605	0.7858
	0.492 (Ar)	0.498 (Ar)	0.511 (Ar)	0.371 (N ₂)	0.376 (N ₂)	0.386 (N ₂)						
	0.891 (Xe)	0.901 (Xe)	0.925 (Xe)									

Note: ^aExpansion to $p_G = 0.01$ torr; Reservoir temperature $T_0 = 300$ K; $y_Q = [QF_6]/[G] \leq 0.05$; $R_{\text{jet}} = 1$ cm; $L = 20$ cm; $\gamma = c_p/c_v$. ^b Throat sonic velocity $U_{\text{st}} = \{2/(\gamma + 1)\}^{1/2} U_{\text{so}}$. Reservoir sonic velocities at $T_0 = 300$ K are: $U_{\text{so}} = 1.0193$ km/s for He; $U_{\text{so}} = 0.322$ km/s for Ar; $U_{\text{so}} = 0.178$ km/s for Xe; $U_{\text{so}} = 1.321$ km/s for H₂; $U_{\text{so}} = 0.353$ km/s for N₂; $U_{\text{so}} = 0.1507$ km/s for SF₆; $U_{\text{so}} = 0.0876$ km/s for SiBr₄. ^c $t_{\text{tr}} = L/\bar{U} = 2L/(U + U_{\text{st}})$, seconds.

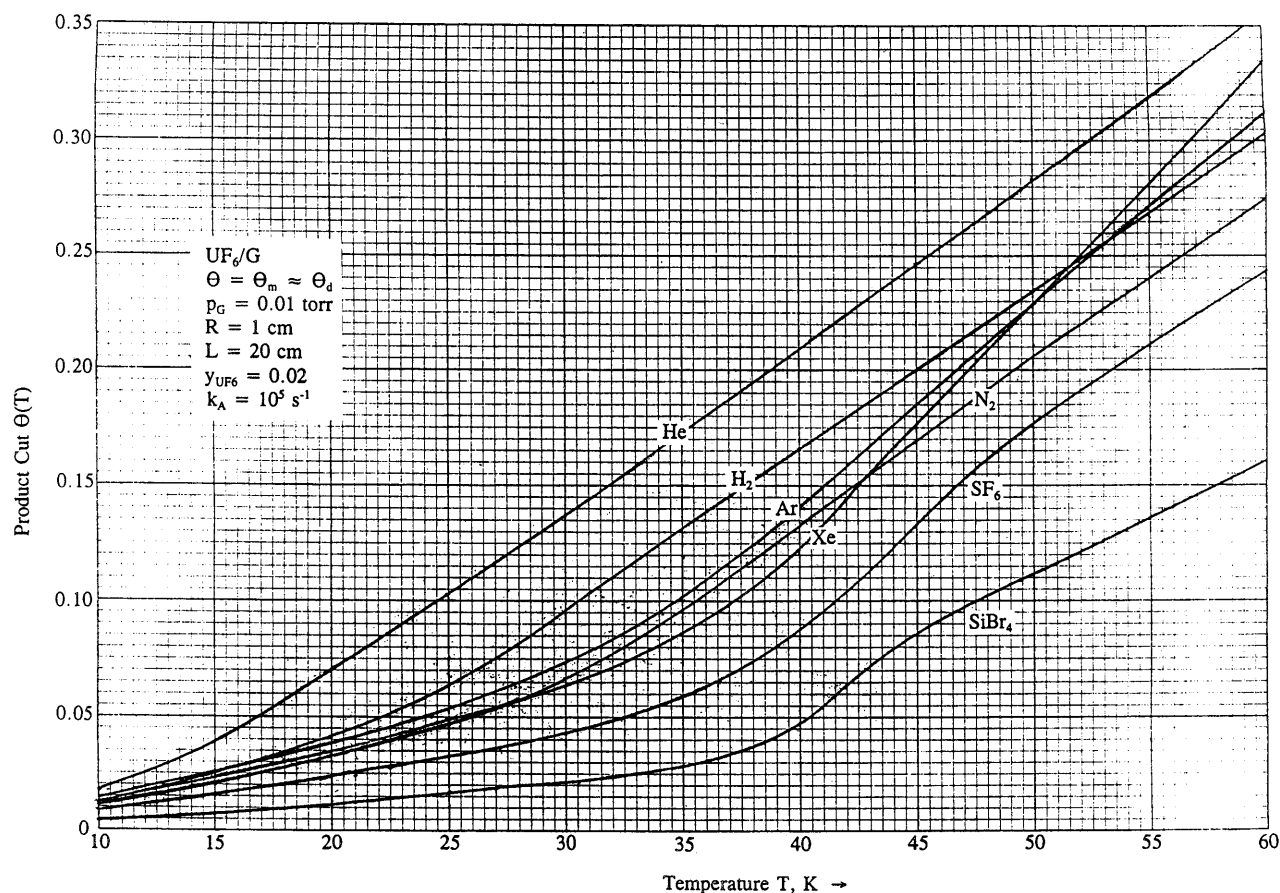


Fig. 9A. Isotope product cuts $\Theta(T)$ for $^{235}\text{UF}_6$ at fixed p_G .

laser beam is passed cross-wise through the free jet (Eerkens, 1998). Pre-expansion of the gas mix through a two-dimensional supersonic slit nozzle is again desirable to tailor the free jet for better laser beam overlap.

7.2. Nucleation and particle growth

To determine whether significant concentrations of $(\text{QF}_6)_N$ clusters could develop during the transit time t_{tr} as the jet expands to the desired final temperature and partial pressure, we examine conditions that cause nucleation. Typically the final partial pressure of QF_6 is $p_Q \sim 2 \times 10^{-4}$ torr if the final gas jet pressure is $p \approx p_G \sim 10^{-2}$ torr and $y_Q = 0.02$. At adiabatic expansion temperatures of $T \leq 100$ K, this pressure p_Q is well above the equilibrium vapor pressure p_{eQ} of both SF_6 and UF_6 (and other QF_6 species) listed in Table 5. Under normal equilibrium this would cause QF_6 to condense, but in the gas phase the process is retarded because of the reduced surface tension (Kelvin effect) and reduced binding energy per monomer of small clusters. The actual pressure p_{dQ} at which QF_6 vapor would start to nucleate and grow $(\text{QF}_6)_N$ clusters in the gas is much higher than p_{eQ} . As reviewed in Eerkens (2003), depending on pressure p_Q and temperature T , a “critical” particle size r_* or monomer loading N_* can be calculated, requiring time t_c

to grow. N -mers with $N < N_*$ do not grow since they can not keep additional monomers on their surface during repeated collisions. That is, all sub-critical N -mers (dimers, trimers, . . .) exist only transiently in extremely small concentrations (Eerkens, 2001a).

At $T > \sim 150$ K, the concentration of dimers at any instant is much lower than that of monomers, while trimer populations are orders-of magnitude smaller than those of dimers, etc. Thus nucleation is of no concern. However for a condensable vapor which is suddenly cooled in an expanding free jet to $T < 100$ K, significant particle (“snow”) formation might occur since $N_*(T)$ drops rapidly as T drops and consequently the concentration of critical N_* -mers can increase steeply. Even then, this can only happen if the time constant t_c for growth is less than t_{tr} ($\sim 10^{-3}$ s). Although heterodimers $\text{QF}_6:\text{Ar}$ and hetero- N -mers $(\text{QF}_6)_N:\text{Ar}_K$ also form, we briefly examine growth of homo- N -mers $(\text{QF}_6)_N$, and assume the results for hetero- NK -mers are similar.

To determine N_* as a function of T and p_Q or $\phi_Q = \ln(p_Q/p_{eQ})$, a quartic equation must be solved, while an estimate of $t_c = t_c(N_*)$ requires analysis of a kinetics rate equation (Eerkens, 2003). Computer-calculated values of $N_*(T)$ for some selected temperatures considered earlier, are listed in Table 5. For a given N_* , t_c can be calculated via the relations (Eerkens, 2003):

Table 5. Calculated nucleation and particle growth parameters for $(QF_6)_N$

Parameter	SF ₆ ($D_\alpha = 180 \text{ cm}^{-1}$; $\epsilon_\alpha = 12.4 \text{ cm}^{-1}$; $\Omega_Q = 127 \text{ \AA}^3$)			UF ₆ ($D_\alpha = 400 \text{ cm}^{-1}$; $\epsilon_\alpha = 9.5 \text{ cm}^{-1}$; $\Omega_Q = 159 \text{ \AA}^3$)		
	T = 10 K	T = 39 K	T = 74 K	T = 10 K	T = 25 K	T = 45 K
p_G , torr	0.01	0.01	0.01	0.01	0.01	0.01
p_Q , torr	2×10^{-4}	2×10^{-4}	2×10^{-4}	2×10^{-4}	2×10^{-4}	2×10^{-4}
p_{eQ} , torr	3.6×10^{-63}	1.9×10^{-23}	5.02×10^{-9}	6.18×10^{-259}	4.27×10^{-98}	7.57×10^{-50}
$\phi_Q = \ell n(p_Q/p_{eQ})$	135.23	43.79	10.59	590.64	215.7	104.6
N_*	2	4	20	2	2	2
Z_{N^*}	0.374	3.86×10^{-2}	1.08×10^{-4}	0.374	0.374	0.374
ϕ_c	4.69×10^{-12}	4.791×10^{-4}	6.013×10^{-3}	7.486×10^{-26}	4.220×10^{-11}	7.297×10^{-7}
$g(D_\alpha, \epsilon_\alpha, T)$	9.87×10^7	135.25	0.252	4.377×10^{20}	1.249×10^5	2.226
n_Q , cm^{-3}	1.94×10^{14}	4.97×10^{13}	2.69×10^{13}	1.94×10^{14}	7.76×10^{13}	4.31×10^{13}
Λ_*	6.106×10^{-26}	5.897×10^{-7}	1.102×10^{-18}	3.301×10^{-64}	1.393×10^{-19}	7.557×10^{-8}
τ_4 , s	2.463×10^3	0.0872	100.1	1.213×10^{13}	133.8	0.2092
t_c (20%), s	1.741×10^3	0.0617	70.8	8.57×10^{12}	94.6	0.1479

$$Z_{N^*} = 2^{7/2} [(N_* - 1)^{1/2} / \{N_*^{10/3} (N_* + 1)\}] \quad (105)$$

$$\phi_c = \{\exp(-D_\alpha/kT)\} \{1 - \exp(-\epsilon_\alpha/kT)\} \quad (106)$$

$$g = [1 - \{1 + \frac{1}{4}\epsilon_\alpha^2/(D_\alpha kT)\} \{\exp(-\frac{1}{4}\epsilon_\alpha^2/(D_\alpha kT))\}] / \phi_c \quad (107)$$

$$\Lambda_* = \phi_c Z_{N^*} g^{-2} \{\ell n(1 + g)\}^{N^*} \approx \phi_c Z_{N^*} g^{N^*-2}, \text{ if } g \ll 1 \quad (108)$$

$$n_Q = 0.97 \times 10^{19} p_Q / T, \text{ cm}^{-3} \quad (109)$$

$$\tau_4 = [1.65 \times 10^{-49} n_Q^4 (T/M_Q)^2 \Omega_Q^{8/3} \Lambda_*]^{-1/4}, \text{ s} \quad (110)$$

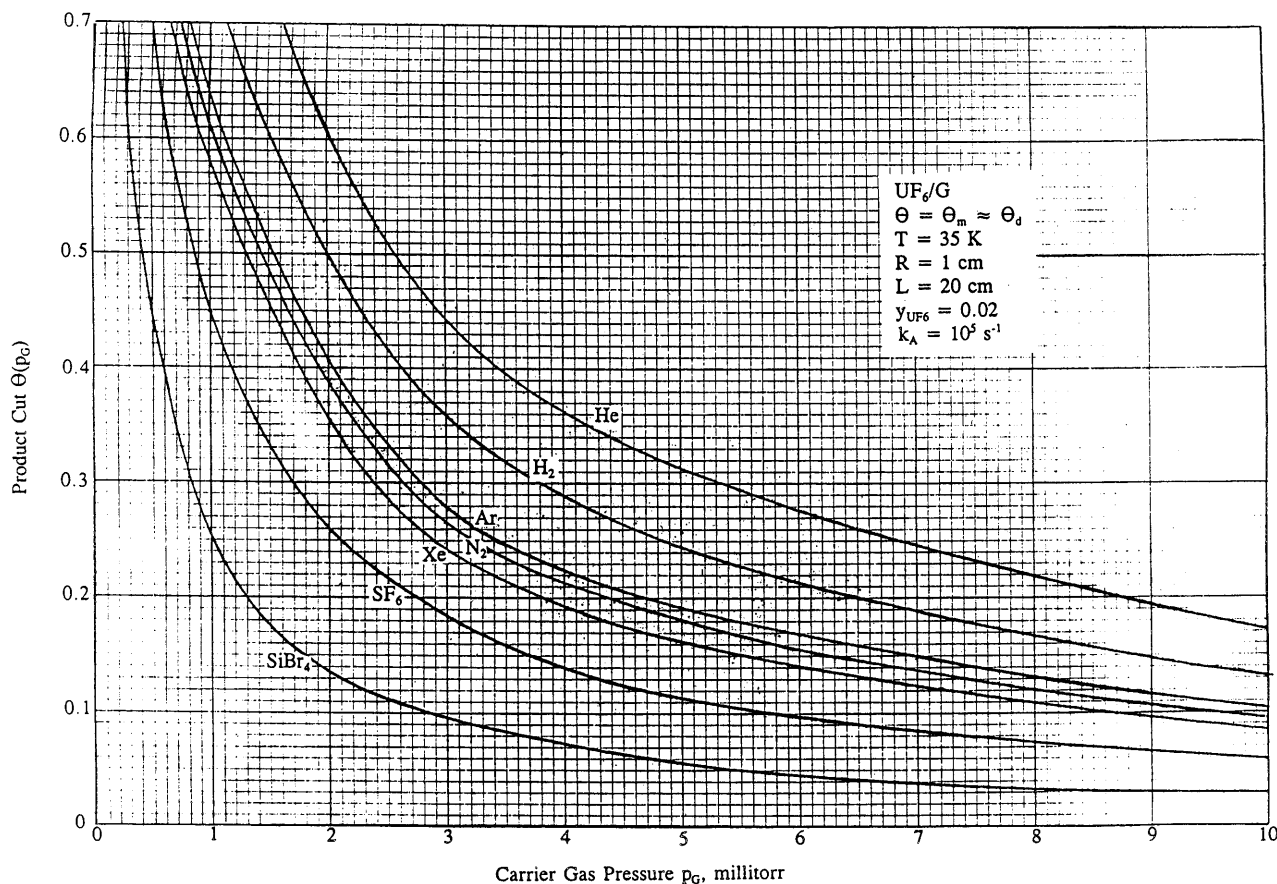


Fig. 9B. Isotope product cuts $\Theta(p_G)$ for $^{235}\text{UF}_6$ at fixed T .

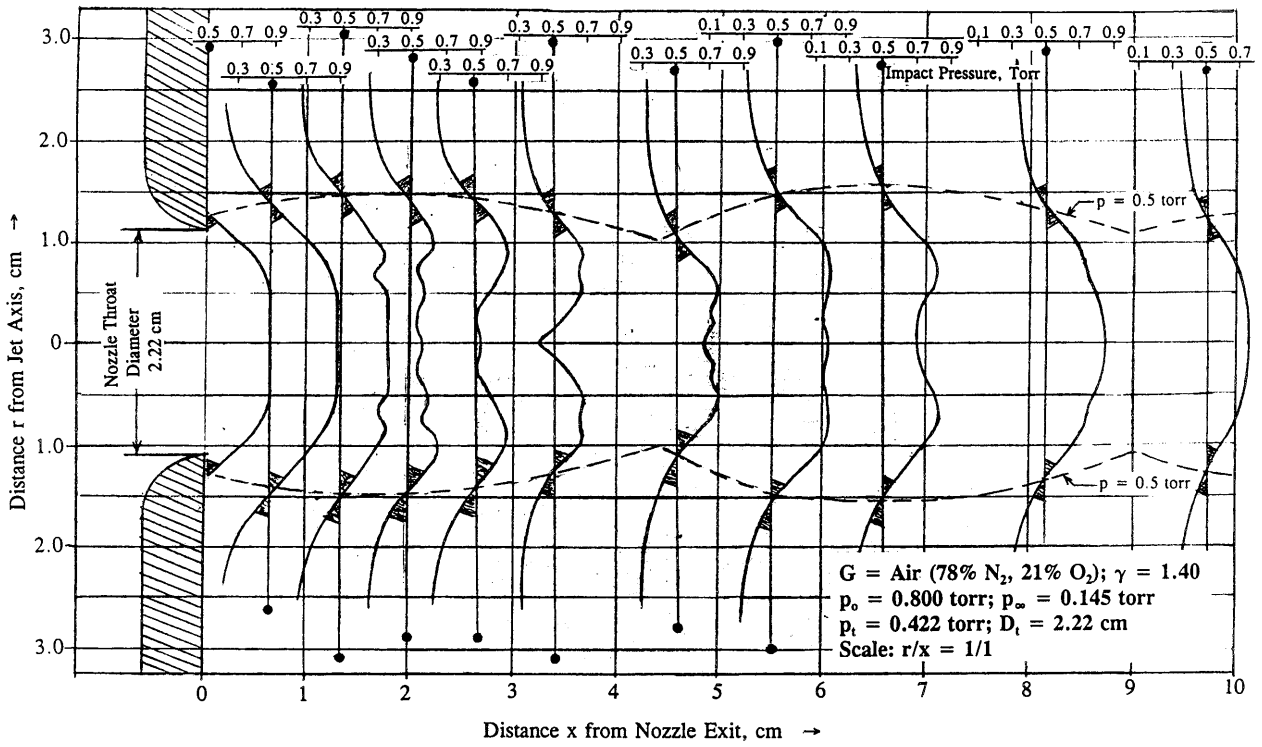


Fig. 10. Measured free-jet contour and pressure distribution for $G = \text{Air}; p_o = 3.86; p_\infty = 0.21 \text{ torr}$ (after Eerkens, 1958; Chow, 1959).

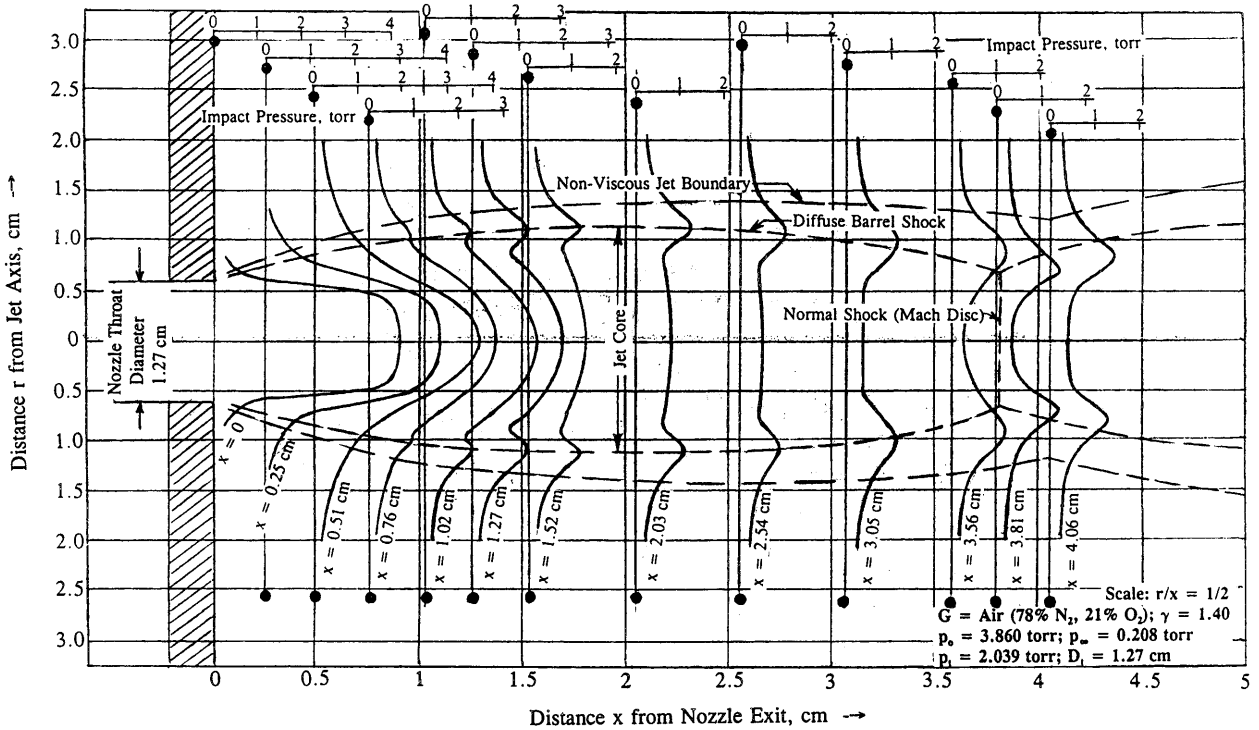


Fig. 11. Measured free-jet contour and pressure distribution for $G = \text{Air}; p_o = 0.80; p_\infty = 0.15 \text{ torr}$ (after Eerkens, 1958; Chow, 1959).

$$t_c = \tau_4(y_c^{-1} - 1)^{1/4} \\ = 0.707 \tau_4 \text{ (for } y_c = 0.8, \text{ i.e. 20\% condensation), s.} \quad (111)$$

Here D_α and ϵ_α are the dimer-bond well-depth and fundamental frequency discussed in Section 3.4, while t_c is the time it takes for 20% of the QF_6 to have condensed into growing particles. Units in Eq. (110) are: T (K), M_Q (amu), n_Q (molecules/cm³), and Ω_Q is the volume of one QF_6 molecule in the condensate in Å³. The latter is readily calculated from the relation:

$$\Omega_Q = 1.66 M_Q(\text{amu})/\rho_Q(\text{g/cm}^3), \text{ \AA}^3/\text{monomer}, \quad (112)$$

where ρ_Q is the density of QF_6 (liquid or solid) condensate, tabulated in Physics Handbooks. Values of D_α , ϵ_α , and Ω_Q for SF_6 and UF_6 are listed in Table 5. Some t_c times calculated by (105)–(111) are tabulated in Table 5, showing the shortest time $t_c \sim 0.1$ s. Thus for jet transit times of $t_{tr} < 10^{-3}$ s and $p_Q < 2 \times 10^{-4}$ torr, there is not enough time for cluster development. However note from (110) that $\tau_4 \propto n_Q^{-1}$ so clustering can occur if $p_Q > 10^{-2}$ torr.

Note from Table 5 that t_c exceed 100 seconds both at high and low temperatures. At high T this is caused by the high value of $N_*(T)$. For example oligomers with $N = 20$, needed to start SF_6 nucleation at $T = 74$ K, are extremely rare and have vanishingly small populations ($< 10^{-80}$ cm⁻³). At temperatures of $T = 10$ K, the high t_c values are due to low collision rates.

8. DISCUSSION AND CONCLUSIONS

To make an isotope separation scheme attractive, one needs a reasonable unit throughput F_{unit} (moles of feed per hour) and energy consumption $E_C = P_e/F_{\text{unit}}$ (kWhr/mole) per separator, besides a good enrichment factor β ($> \sim 1.8$), high Θ_o ($> \sim 0.08$), and low γ ($< \sim 0.93$). There are many isotope separation processes (e.g., calutrons) with high β 's but low F_{unit} and high E_C which are uneconomic compared to other separation methods.

Our analyses showed that to achieve high CRISLA enrichment factors β with good cuts Θ_o , operating pressures of less than 0.1 torr are necessary. If $p_G \approx p_{\text{tot}} \sim 10^{-2}$ torr, the QF_6 partial pressure in the jet core is only $p_Q \sim 2 \times 10^{-4}$ torr if $y_Q = 0.02$ (to minimize VV losses). This compares with pressures of 2×10^{-5} torr used in electromagnetic calutron isotope enrichments, whose economics is poor compared to ultracentrifuge isotope separations (presently the favored non-laser method) because of low throughputs. Fortunately a free jet moves at supersonic velocities (as do ions in a calutron) which partially off-sets low operating pressures.

With supersonic velocities of $\bar{U} \sim 3 \times 10^4$ cm/s, QF_6 feed through-puts will be on the order of 2.5×10^4 cm³/s per separator or approximately 0.01 moles/hr, if $p_Q = 2 \times 10^{-4}$ torr, $T = 25$ K, assuming a single axisymmetric jet with

(average) radius $R = 0.5$ cm. For small-quantity isotope productions needed in nuclear medicine, this rate is adequate. For larger scale operations the rate per separator can be substantially increased by utilizing two-dimensional slit nozzles and free-jets which are laser-irradiated cross-wise (Eerkens, 1998).

An advantage of laser isotope separation schemes over calutrons and other mass-action methods is that in the laser case, energy only needs to be spent on a specific isotopomer, whereas in calutrons the electron discharge must ionize every isotope of the atomic element. Also, excluding preparation and other losses, only ~ 0.1 eV per desired isotope is spent in CRISLA, instead of ~ 6 eV to ionize every isotope of the element in calutron separations. Thus a laser scheme can save energy if laser photon generation is efficient.

As mentioned, another advantage of the CRISLA process with free-jet harvesting is that feed and product streams are the same gas. Chemical reprocessing of products or tails as required in other MLIS schemes, is absent. Thus several enriching stages can be put directly in series in CRISLA to produce the desired final level of isotope enrichment.

In the analyses, it was tacitly assumed that hetero-dimers ${}^i\text{QF}_6^*:\text{G}$ provided the main source of isotope-enriching epithermal ${}^i\text{QF}_6^!$ molecules. Homo-dimers ${}^i\text{QF}_6^*:\text{QF}_6$ also form and after predissociation could give high kinetic energies after VT conversion (see Eq. 42). However for ${}^i\text{QF}_6^*:\text{QF}_6$ homo-dimers there is a high probability for VV transfer and isotope-scrambling prior to predissociation. This diminishes isotope enrichment and is undesirable. To minimize VV transfers, concentrations y_Q of QF_6 in the carrier gas are kept low ($y_Q < \sim 0.05$).

Because the mole fraction y_Q of QF_6 in carrier gas G is low, and a low abundance x_i of laser-irradiated isotope ${}^i\text{Q}$ makes the concentration $y_Q x_i$ even lower, another tacit assumption made was that the absorbed and VT-released laser energy is insufficient to heat jet gases. If x_i and/or y_Q are high, laser heating of the jet gases might have to be considered. In most practical cases however, $y_Q x_i \ll 1$ and this effect can be ignored.

It might appear desirable to have high ${}^i\text{QF}_6^!$ escape factors and thus to have the collision mean-free-path ℓ_c be on the order of the jet core radius R_j . However with $\ell_c \sim R_j$, one would have nearly collisionless slip-flow and Knudsen-regime conditions. This would preclude enough collisions of ${}^i\text{QF}_6^*$ with G to produce an adequate population of ${}^i\text{QF}_6^*:\text{G}$ species for achieving isotope separation. The optimum gas pressures for isotope separation are thus in the low-pressure region of continuum fluid mechanics, where gaseous diffusion relations are still valid.

According to (42), a carrier gas G with high mass M_G gives the highest kinetic energy to ${}^i\text{QF}_6$ and yields the highest β 's, provided G does not possess any internal vibrations with a frequency close to ν_3 of QF_6 . Thus use of heavy carrier gases such as Br_2 ($M = 160$), SiCl_4 ($M = 172$), SiBr_4 ($M = 348$), whose vapor pressures still exceed 10 torr at

room temperature, might appear advantageous at first glance. However Table 4 shows that a very low value of γ (e.g., $\gamma = 1.07$ for SiBr_4) requires impossibly high reservoir pressures and small nozzle throat diameters. This suggests use of a three-component gas mixtures such as $\text{QF}_6 + \text{Ar} + \text{SiBr}_4$ studied in earlier CRISLA experiments (Eerkens, 1998; Eerkens *et al.*, 1995, 1996). The effect of two carrier gases G_1 and G_2 on β and Θ_0 of ${}^i\text{QF}_6$ will be left to a future study.

Noble gases would be most convenient as carrier gases but do not yield the very highest enrichments. Xe gives the highest β 's of all noble gas carriers because of its high mass ($M = 131$) and favorable γ ($= 1.67$), but it is rather expensive. SF_6 ($M = 146$) as carrier gas is less expensive and with $\gamma = 1.33$ is still usable for supersonic expansions according to Table 4. Thus for UF_6 enrichments, carrier gas SF_6 is preferred, provided VV transfers of UF_6 's ν_3 quanta at 628 cm^{-1} to SF_6 's ν_4 vibration at 616 cm^{-1} are minor. The advantage of SF_6 is also that it can be cryo-pumped. At 77 K (liquid N_2), the vapor pressure of SF_6 is on the order of 10^{-5} torr, precisely the desired sink pressure for evacuating rim gases from the free-jet chamber.

Note that direct epithermal escapes are mostly operative in the outer region of the jet core at a distance $\bar{s}_{\text{th}} \sim 1.41 N_T^{1/2} \ell_c$ from the imaginary "wall" (see Eq (53)). Thus at higher pressures where ℓ_c is small, only laser excitations in the annular region between $(R - \bar{s}_{\text{th}})$ and R of the jet core donate high-speed core-fleeing isotopomers directly. In the laser-illuminated interior of the jet core, most epithermals are slowed down before they can reach the jet "wall." In the interior region, the main contribution to isotope separation comes from non-excited isotopomers ${}^i\text{QF}_6$ which form long-lived heavy ${}^i\text{QF}_6\text{:G}$ dimers. These dimers migrate more slowly than laser-excitable ${}^i\text{QF}_6$ monomers which migrate faster at monomer (thermal or epi-thermal) speeds.

Of course the calculated β 's in Figures 3 through 6 are only estimates because of mathematical approximations and uncertainties in the values of some physical constants. Nevertheless the theory should predict trends correctly and provide useful approximate values of enrichment factors needed for the design of CRISLA separators. Though we focussed on ${}^{33}\text{SF}_6$ and ${}^{235}\text{UF}_6$ isotope separations, the equations can be used equally well for ${}^{123}\text{TeF}_6$ and ${}^{98}\text{MoF}_6$ or any other ${}^i\text{QF}_6$ or ${}^i\text{QX}_m\text{Y}_n$ isotopomer, assuming lasers with suitable frequencies are available.

ACKNOWLEDGMENTS

I am indebted to Dr. W.H. Miller at the University of Missouri (MU) for programming the computer-calculated curves of Figs 2 through 9. To former MU student Dr. Jaewoo Kim, I am grateful for performing some of the experiments that led me to investigate and re-examine condensation repression physics in free jets. I also wish to thank Dr. S. Loyalka, Dr. W.H. Miller, and Dr. M.A. Prelas at MU, as well as Dr. J.F. Kunze at Idaho State University for valuable discussions and support of my laser isotope separation research.

REFERENCES

- ADAMSON, T.C. & NICHOLS, J.A. (1959). On the structure of jets from highly underexpanded nozzles into still air. *J. Aerospace Sciences* **1**, 23.
- BENEDICT, M., PIGFORD, T.H. & LEVI, H. (1981). *Nuclear Chemical Engineering*, 2nd Edition, New York, McGraw-Hill.
- BERNSTEIN, L.S. & KOLB, C.E. (1979). Understanding the IR continuum spectrum of the N_2O dimer and other VanderWaals complexes at low temp's. *J. Chem. Phys.* **71**.
- BESWICK, J.A. & JORTNER, J. (1978). Perpendicular vibrational predissociation of t-shaped VanderWaals molecules. *J. Chem. Phys.* **69**, 512.
- BEU, T.A. & TAKEUCHI, K. (1995). Structure and IR-spectrum calculations for small SF_6 clusters. *J. Chem. Phys.* **103**, 6394.
- BEU, T.A., ONOE, J. & TAKEUCHI, K. (1997). Calculations of structure and IR-spectrum for small UF_6 clusters. *J. Chem. Phys.* **106**, 5910.
- BURAK, I., HOUSTON, P., SUTTON, D.G. & STEINFELD, J.I. (1970). Observation of laser-induced acoustic waves in SF_6 . *J. Chem. Phys.* **53**, 9.
- CHOW, R.R. (1959). On the separation of a binary gas mixture in an axisymmetric jet. Tech Report HE-150-175 (Series 110, Issue No. 5) University of California-Berkeley, Institute of Engineering Research.
- EERKENS, J.W. (1957a). Design considerations and region of operation of the jet diffusion equipment. Tech Report HE-150-158 (Series 110, Issue No. 3) University of California-Berkeley, Institute of Engineering Research.
- EERKENS, J.W. & GROSSMAN, L.M. (1957b). Evaluation of the diffusion equation and tabulation of experimental gaseous diffusion constants. Tech Report HE-150-150 (Series 110, Issue No. 1). University of California-Berkeley, Institute of Engineering Research.
- EERKENS, J.W., SEHGAL, B. & GROSSMAN, L.M. (1958). Some preliminary results on the separation of gaseous components in a jet. Tech Report HE-150-162 (Series 110, Issue No. 4). University of California-Berkeley, Institute of Engineering Research.
- EERKENS, J.W. (1973). *Model equations for photon emission rates and absorption cross-sections (Rocket Radiation Handbook Volume II)*, USAF-FTD-CW-01-01-74, AD-A007946.
- EERKENS, J.W., KUNZE, J.F. & ANDERSON, G. (1995). Mo-98 and Mo-99 laser isotope separation for nuclear medicine. *Proc. Missouri Ac. of Science, Eng'ng Section*.
- EERKENS, J.W., MILLER, W.H. & PUGLISI, D. (1996). Laser separation of medical isotopes— QF_5Cl Spectra. ANS Transactions of Nov. 11–14, 1996, Washington DC Meeting.
- EERKENS, J.W. (1998). Separation of isotopes by laser-assisted retardation of condensation (SILARC). *Laser Part. Beams* **16**, 295.
- EERKENS, J.W. (2001a). Equilibrium dimer concentrations in gases and gas mixtures. *Chem. Phys.* **269**, 189.
- EERKENS, J.W. (2001b). Average diffusion-to-the-wall times for laser-tagged molecules in a long cylinder. *Appl. Phys. B* **72**, 885.
- EERKENS, J.W. (2003). Nucleation and particle growth in supercooled flows of SF_6/N_2 and UF_6/N_2 mixtures. *Chem. Phys.* **293**, 111–153.
- EERKENS, J.W. (2005). Condensation reduction and isotope separation of laser-excited molecules in wall-cooled subsonic gas streams, *Nucl. Sci. Eng.* **150**, 1–22.

- GERAEDTS, J., SETIADI, S., STOLTE, S. & REUSS, J. (1981). Laser induced predissociation of SF₆ clusters. *Chem. Phys. Let.* **78**, 277.
- GERAEDTS, J., STOLTE, S. & REUSS, J. (1982). Vibrational predissociation of SF₆ dimers and trimers. *Z. Physik A* **304**, 167–175.
- GLASSTONE, S. & EDLUND, M.C. (1952). *The elements of nuclear reactor theory*, Chapter 6; New York: Van Nostrand.
- HERZBERG, G. (1945). *Infrared and raman spectra*, New York: Van Nostrand.
- HIRSCHFELDER, J.O., CURTISS, C.F. & BIRD, R.B. (1967). *Molecular Theory of Gases and Liquids*. Footnote on page 555 of Section 4a; John Wiley New York, Fourth Printing 1967.
- KIM, K.C. & PERSON, W.B. (1981). Study of absolute IR intensity of ν_3 absorption of UF₆. *J. Chem. Phys.* **74**, 171.
- KRAUS, M. (1967). *Compendium of ab initio Calculations of Molecular Energies and Properties*, National Bureau of Standards, Technical Note NBS TN 438, Dec 1967, US Government Printing Office, Washington DC.
- LEE, Y.T. (1977). Isotope separation by photodissociation of VanderWaals molecules. U.S. Patent 4,032,306, issued June 1977.
- LIEDENBAUM, C., HEIJMEN, B., STOLTE, S. & REUSS, J. (1989). IR predissociation of halogenated methane VanderWaals complexes. *Z. Physik D* **11**, 175–180.
- LIEPMANN, H.W. & PUCKETT, A.E. (1953). *Introduction to Aerodynamics of a Compressible Fluid*, Ronald Press (1953).
- MCCAFFEREY, A.J. & MARSH, R.J. (2002). Vibrational predissociation of vanderWaals molecules; An internal collision, angular momentum model. *J. Chem Phys.* **117**, 9275.
- SCHWARTZ, R.N., SLAWSKI, Z.I. & HERZFELD, K.F. (1952). Calculation of vibrational relaxation times in gases. *J. Chem. Phys.* **20**, 159.
- SCHWARTZ, R.N. & HERZFELD, K.F. (1954). Vibrational relaxation times in gases (three-dimensional treatment). *J. Chem. Phys.* **22**, 5.
- SMALLEY, R.E., LEVY, D.H. & WHARTON, L. (1976). The fluorescence excitation spectrum of the HeI₂ VanderWaals complex. *J. Chem. Phys.* **64**, 3266.
- SNELLS, M. & REUSS, J. (1987). Induction effects on IR-predissociation spectra of (SF₆)₂, (SiF₄)₂, and (SiH₄)₂. *Chem. Phys. Let.* **140**, 543.
- VANBLADEL, J.W.I. & VANDERAVOIRD, A. (1990). The infrared photodissociation spectra and the internal mobility of SF₆, SiF₄, and SiH₄ dimers. *J. Chem. Phys.* **92**, 2837.
- VANDENBERGH, H. (1985). Laser assisted aerodynamic isotope separation," *Laser und Optoelektronik* **3**, 263.
- YARDLEY, J.T. (1980). *Introduction to Molecular Energy Transfer*, Academic Press New York, 1980.